Deep Learning based Automated Diagnosis of Ocular Toxoplasmosis in Fundus Images using Convolutional Neural Network

by

Prionto Kumar Choudhury
19301089
Asma Akter Anika
19301038
Sumaiya Rahman Ramisa
19301147
Arsi Zaman
19301103
Rizvee Rifat Chowdhury
19101502

A thesis submitted to the Department of Computer Science and Engineering
in partial fulfillment of the requirements for the degree of
B.Sc. in Computer Science and Engineering

Department of Computer Science and Engineering
School of Data and Sciences
BRAC University
January 2024

Declaration

It is hereby declared that

1. The thesis submitted is our own original work while completing degree at Brac University.
2. The thesis does not contain material previously published or written by a third party, except where this is appropriately cited through full and accurate referencing.
3. The thesis does not contain material which has been accepted, or submitted, for any other degree or diploma at a university or other institution.
4. We have acknowledged all main sources of help.

Student's Full Name & Signature:

Prionto Kumar Choudhury

Prionto Kumar Choudhury
19301089

Sumaiya Rahman Ramisa

Sumaiya Rahman Ramisa
19301147

Asma Akter Anika

Asma Akter Anika
19301038

Arsi Zaman

Arsi Zaman
19301103

Rizvee Rifat Chowdhury

Rizvee Rifat Chowdhury
19101502

Approval

The thesis titled "Deep Learning Based Automated Diagnosis of Ocular Toxoplasmosis in Fundus Images Using Convolutional Neural Network" submitted by

1. Prionto Kumar Choudhury (19301089)
2. Asma Akter Anika (19301038)
3. Sumaiya Rahman Ramisa (19301147)
4. Arsi Zaman (19301103)
5. Rizvee Rifat Chowdhury (19101502)

Fall 2023 has been accepted as satisfactory in partial fulfillment of the requirement for the degree of B.Sc. in Computer Science on 18 January, 2024.

Examining Committee:

Supervisor:

(Member)

Dr. Md.Golam Rabiul Alam
Professor
Department of Computer Science and Engineering
BRAC University

Co-Supervisor:

(Member)

MD. Tanzim Reza
Lecturer
Department of Computer Science and Engineering
BRAC University

Program Coordinator:

(Member)

Dr. Md Golam Rabiul Alam
Professor
Department of Computer Science and Engineering
BRAC University

Head of Department:

(Chair)

Dr. Sadia Hamid Kazi
Chairperson and Associate Professor
Department of Computer Science and Engineering
BRAC University

Abstract

Ocular toxoplasmosis (OT) is often diagnosed by a specialist by the examination of fundus images of the eye. While deep learning is commonly used to process and identify diseases in medical images, ocular toxoplasmosis (OT) diagnosis has not received much attention up to this point.. We created and applied an effective Convolutional Neural Network (CNN) model that can accurately detect and classify Ocular Toxoplasmosis (OT) photos into four different groups: healthy, active, inactive, active-inactive. Later on, except healthy, three other classes turned to be an one class which is unhealthy. We created and applied an effective Convolutional Neural Network (CNN) model that can accurately detect and classify Ocular Toxoplasmosis (OT) photos into two different groups which are Healthy and Unhealthy. We claimed a proposed model that can accurately recognize and distinguish between the OT pictures on binary classes. In order to demonstrate the effectiveness of our customised Convolutional Neural Network (CNN) model, we employed four pre-trained models (VGG-16, VGG-19, MobileNet, ResNet50) and evaluated them using the same dataset. Our proposed custom model, along with four pretrained CNN architectures, demonstrates similar performance on the available dataset in terms of accuracy, precision, recall, and f1 score, as evaluated in this research. The proposed model shows a 95% accuracy rate. The CNN model recommended for diagnosing retinal disorders outperforms all previously utilised model.
Keywords: Ocular Toxoplasmosis; Deep Learning; Convolutional Neural Network; VGG-19; ResNet50; VGG-16; MobileNet.

Acknowledgement

We begin by expressing our gratitude to the Almighty Allah for preserving our physical and mental well-being, allowing us to execute our thesis work titled " Deep Learning based Automated Diagnosis of Ocular Toxoplasmosis in Fundus Images using Convolutional Neural Network " seamlessly and within the designated time frame. We also acknowledge the divine endowment of knowledge, skills, and determination that empowered us to accomplish our task.

Our heartfelt appreciation goes out to our dedicated supervisor, Dr.Md.Golam Rabiul Alam, PhD, an Professor in Computer Science and Engineering and Tanzim Reza sir for their invaluable guidance, unwavering support, continuous motivation, and constructive suggestions throughout our thesis journey. His enduring assistance has been instrumental in comprehensively developing our work and ideas.

The successful outcome of this study is not solely the result of individual toil, but rather a product of the collective efforts of numerous individuals. We extend our gratitude to our parents, whose unwavering hope and ongoing support have enabled us to pursue our career aspirations. Without their unwavering support, completing our thesis work would have been an uphill battle.

Table of Contents

List of Figures

List of Tables

Nomenclature

The next list describes several symbols & abbreviation that will be later used within the body of the document

CNN Convolutional Neural Network

CV Computer Vision

$LSTM$ Long Short Term Memory

NLP Natural Language Processing

OT Ocular Toxoplasmosis

$RMSprop$ Root Mean Square propagation

SGD Stochastic Gradient Descent

$T.gondii$ Toxoplasma gondii

TP True Positive

VGG Visual Geometry Group

Chapter 1

Introduction

Ocular toxoplasmosis, caused by Toxoplasma gondii, is a significant eye infection with potential risks to vision. It is broadly classified into congenital and acquired forms, the former arising from maternal-fetal transmission and the latter from contaminated food or water. It's a common obligate intercellular parasite that spreads throughout nature and creates a zoonotic threat to both humans and warm-blooded animals. Globally, an estimated one-third of people are thought to have a persistent T. gondii infection. On the other hand, different geographic regions with distinct toxoplasmic environments—that is, distinct climates, dietary practices, and levels of hygiene—have differing disease prevalence and infection sources.

Research suggests that millions of people worldwide encounter ocular toxoplasmosis annually. Toxoplasmic retinochoroiditis, which accounts for 30–55% of posterior uveitis, is the primary cause of visual impairment in high-endemic T. gondii regions of the United States and Europe [11].For a long time, it was believed that ocular toxoplasmosis was caused by the congenital form of the disease returning. The idea that acquired infections rather than congenital ones may be a more significant cause of ocular disorders is, nevertheless, supported by more recent reports.

Auto diagnosis system by computer is preferable now to quickly spot different ocular toxoplasmosis signs in eye pictures, just like skilled eye doctors do with retinal scans.The primary diagnostic approach involves inspecting distinct abnormalities fundus photographs. Deep learning, particularly Convolutional Neural Networks (CNNs), has significantly advanced disease understanding in the medical field. CNNs utilize fundus images to measure the likelihood of ocular toxoplasmosis and generate a heatmap highlighting the indicative region. Identification of ocular toxoplasmosis prompts further specification based on the dataset.Its depend on how large the data set is then the result will be more accurate.We will apply random changes to the test sets, validation dataset, and training dataset in the Ocular Toxoplasmosis Detection Challenge in order to ensure their independence. In order to generate more accurate results in the image there will be two classes healthy and unhealthy.We will train the dataset in custom model and ensemble model to get more better results than than the pre-trained existing model.

1.1 Motivation

Our research is motivated by the urgent need to enhance ocular toxoplasmosis disease detection through advanced deep learning techniques.The disease's prevalence and impact on ocular health highlight the need for efficient detection methods.However, existing studies have left critical gaps in our understanding of efficient detection methods, particularly in the realm of deep learning for ocular toxoplasmosis. This paper aims to bridge these gaps by developing and implementing innovative deep learning models for accurate disease detection. Through this research, we aspire to contribute crucial insights to ophthalmology and address the current limitations in ocular toxoplasmosis detection knowledge.

1.2 Problem Statement

Ocular toxoplasmosis is a popular and possibly harmful ocular infection that has been linked to the protozoan parasite Toxoplasma gondii.Because ocular toxoplasmosis is a self-limiting condition, several medical professionals refuse to treat minor peripheral lesions. The treatment's objectives are to reduce damage to the optic disc and retina while stopping parasite growth during the active phase of retinochoroiditis[3] [9]. The quick and precise diagnosis of this condition is required for the successful execution of efficient treatments and for the betterment of patient outcomes.Antibodies against T. gondii are mainly important for verifying previous exposures, as seropositivity to the parasite is rather prevalent worldwide. With this seropositive result, however, ocular toxoplasmosis cannot be diagnosed [4].Localized necrotizing retinitis is ocular toxoplasmosis' most typical symptom. It is usually associated with vitritis and commonly coexists with anterior uveitis. Rarely it may appear as papillitis. The earliest noticeable symptoms of ocular toxoplasmosis often appear in the second decade of life. The 5-year recurrence rate in a long-term follow-up was 79%, and some patients had multiple recurrences[2][1]. A slight anterior chamber reaction can be the basis for a severe case of anterior uveitis covering posterior segment disease. Granulomatous or non-granulomatous inflammations are both possible. Moreover, retinochoroiditis may cause significant anterior inflammation around the ora serrata, which is missed on initial tests [6] [7] .Children with congenital toxoplasmosis may acquire cataracts as a consequence of retinochoroiditis or as a follow-up to severe iridocyclitis. Children with cataracts may need to have the cataract surgically removed if they develop significant amblyopia [5]. Near the active retinochoroiditis lesion, the vitreous inflammation is usually more severe. Severe vitritis can cause vitreoretinal tension and the development of epiretinal membranes adjacent to the affected area. "Headlight in the fog" describes the dazzling white reaction that appears when light is directed into the back of the eye using an indirect ophthalmoscope. Severe vitritis is the etiology of this illness. However, the manual analysis of fundus pictures to identify lesions related to toxoplasmosis can be a laborious process that is prone to human error. Hence, there is a need for an automated and capable diagnostic system that is capable of precisely identifying ocular toxoplasmosis lesions in images of the fundus. The main objective are given below.

1.3 Research Objective

Our major goal is to establish a model that automates diagnostics for Ocular Toxoplasmosis in Fundus Images applying Deep Learning and Convolutional Neural Network (CNN) technology. This study intends to address the challenges of manual diagnosis, such as individuality and complicated analysis, by employing deep learning algorithms.
The study's objective emphasizes on building an extensive set of fundus images that includes both healthy eyes and eyes affected by toxoplasmosis. It will develop and optimize a CNN model for precise detection and diagnosis of ocular toxoplasmosis lesions. The system will prioritize accomplishing high levels of sensitivity and specificity in order to minimize the chance of false positives and false negatives.
The automated system will offer early detection and precise localization of ocular toxoplasmosis lesions, enabling intervention in a timely manner. Additionally, this study looks at techniques for monitoring the progression of diseases over a period of time by utilizing long-term fundus image data.
The CNN model will undergo an in-depth assessment using suitable metrics and cross validation techniques. It will be compared to manual diagnoses carried out by experienced ophthalmologists. The model's decisions will be increased to enhance interpret ability and explain ability, which will give information regarding lesion identification.
The study investigates the potential integration of genetic data and electronic medical records for personalized therapy recommendations. Data privacy and regulatory compliance will be considered for potential clinical implementation.
The study is academically significant as it contributes to the fields of ophthalmology and medical imaging by demonstrating the efficacy as well as practicality of using Deep Learning based Automated Diagnosis for Ocular Toxoplasmosis. The possible effect of the automated system on ocular toxoplasmosis diagnosis and management is significant, as it can enhance accuracy, efficiency, and interpret ability. This possesses the potential of resulting in improved patient care and outcomes. The research aims to achieve the following objectives:

1. Acquire a thorough understanding of the fundamental mechanisms of picture processing.
2. understanding pre-processing methods for data, like reshaping and denoising.
3. constructing a model for identifying retinal illness using OT pictures.
4. comprehending the influence of deep learning on our model.
5. offering ophthalmologists clear and precise instructions and assistance in order to expedite and enhance the accuracy of illness detection.

1.4 Paper Orientation

The main purpose of this chaptesr is to enlighten the scholar about toxoplasmosis. It briefly outlines the study's objectives and problem description.The essay's remaining sections are organized as follows: The background material for this investigation is

outlined in Chapter 2, along with the concept of CNN and an explanation of why it is suitable for this research.Chapter 3 contains a literature review of a few prior research that classified healthy and unhealthy tissues in toxoplasmosis patients using ML and DL. The data set, its analysis, its reprocessing, Model Evaluation for use in the study are the main topics of Chapter 4. Chapter 5 of this article presents an introduction to the models utilized in the study, while Chapter 6 delves into a thorough examination of their findings and conclusions.

Chapter 2

Background

2.1 Toxoplasmosis

Toxoplasmosis is a parasitic illness caused by the protozoan worm Toxoplasma gondii. Globally, Toxoplasma gondii (T. gondii) infection is very common. According to research in the United States it is estimited that 11% of the population of more than 6 years are more likely getting affected with ocular toxoplasmosis [12].In various places of world it have shown that around 60% of some population have been infected with toxoplasma.This parasite is responsible of infecting a vast number of warm blooded animals, like humans [12].The primary host for Toxoplasma gondii is the cat and the infection is commonly associated with exposure to cat feces.Furthermore,the parasite can also be transmitted through comsumption of contaminated food,water or undercook meat.

2.2 Toxoplasmosis Life Cycles

The single-celled protozoan parasite Toxoplasma gondii is the source of the parasitic infection known as toxoplasmosis. Numerous warm-blooded species, including humans, are susceptible to infection [22][10] .T. gondii has both asexual and sexual phases in its life cycle, and it usually rotates between definitive and intermediate hosts. The Felidae family, which includes cats mostly, is the definitive host for T. gondii, where sexual reproduction takes place. Oocysts excreted in the faeces of infected cats or tissues consumed by infected animals are the means by which intermediate hosts, including as humans and other warm-blooded animals, become infected [36].

The life cycle of Toxoplasma gondii is summarised as follows:
The Final Host (Cat): The cat's small intestine is where sexual reproduction takes place. Cat excrement contains oocysts, which include sporozoites.
Environment: Oocysts in the natural world can spread disease for several months or even years[36].
Intermediate Hosts: Humans and other warm-blooded animals are intermediate hosts. Ingestion of oocysts by food, drink, or contaminated soil. Ingestion of tissue cysts in undercooked or raw meat carrying T. gondii bradyzoites.
Stage of Tachyzoites (Asexual Reproduction): Sporozoites are discharged and change into tachyzoites following ingestion. Tachyzoites proliferate quickly in a

variety of tissues.
Chronic Infection: Bradyzoites develop into tamachyzoites, which then produce tissue cysts. The individual may have these cysts for the duration of their life.
Return Transmission to the Final Host: When an intermediate host is consumed by a cat, the life cycle restarts with sexual reproduction in the cat's intestines..

2.2.1 Sexual Stage

Toxoplasma gondii's sexual stage is limited to the definitive host, which is mostly domestic cats and other members of the Felidae family [24]. T. gondii reproduces in the small intestine of cats during the sexual stage. The sexual stage of the Toxoplasma gondii life cycle is described in the steps below:

Oocyst Shedding: Cat intestine lining is where mature sexual forms of the parasite called gametocytes develop. Male microgametes and female macrogametes are produced from these gametocytes. Zygotes are created when macrogametes are fertilised by microgametes [24].

Oocyst Formation: After the zygotes continue to develop, oocysts are created.The parasite's infectious form, sporozoites, are found within the protective structures known as oocysts .

Oocyst Shedding in Faeces: Cat faeces contains oocysts that shed[26] . It is through this shedding that infected oocysts infect the environment.Environmental Persistence: Depending on the surroundings, oocysts released into the environment may continue to spread disease for several months or even years.

Transmission to Intermediate Hosts: Oocysts are contracted by eating them through contaminated food, drink, or soil. Intermediate hosts include humans and other warm-blooded animals. The asexual stage of the T. gondii life cycle, which involves the production of tachyzoites and the generation of tissue cysts, starts once the oocysts are consumed by the intermediate host [24].
It's denied to claim that the majority of human infections are caused by oocysts or tissue cysts that are consumed through contaminated food or water. Additionally, the sexual stage only occurs in the final host, the cat. Since it enables the parasite to procreate and complete its life cycle, the sexual stage of Toxoplasma gondii is crucial to its completion.

2.2.2 Asexual Stage

Oocysts produced in cat feces or under cooked meat harboring tissue cysts containing the parasite are the two main ways that the parasite is transmitted to intermediate hosts [24]. The oocysts released when an intermediate host consumes them from contaminated food, water, or soil produce bradyzoites that enter the host's cells.
Tachyzoite Stage: These bradyzoites subsequently go through a number of asexual divisions and become tachyzoites. The parasite's quickly reproducing form is known as a tachyzoite. Tachyzoites can spread throughout the body, infecting the host's tissues severely.

Formation of tissue Cysts: In this stage, healthy people may experience very mild flu-like symptoms or none at all[26]. The infection, however, can be serious and even lethal in those with compromised immune systems or while pregnant. Some of the tachyzoites have the ability to develop into cyst-forming bradyzoites in reaction to the immune system of the host[10] .
Chronic Infection: These cysts are exceptionally hardy and can survive in the host's tissues, notably in the muscles and brain. Latent toxoplasmosis is the name for this persistent, dormant stage of the infection [24].

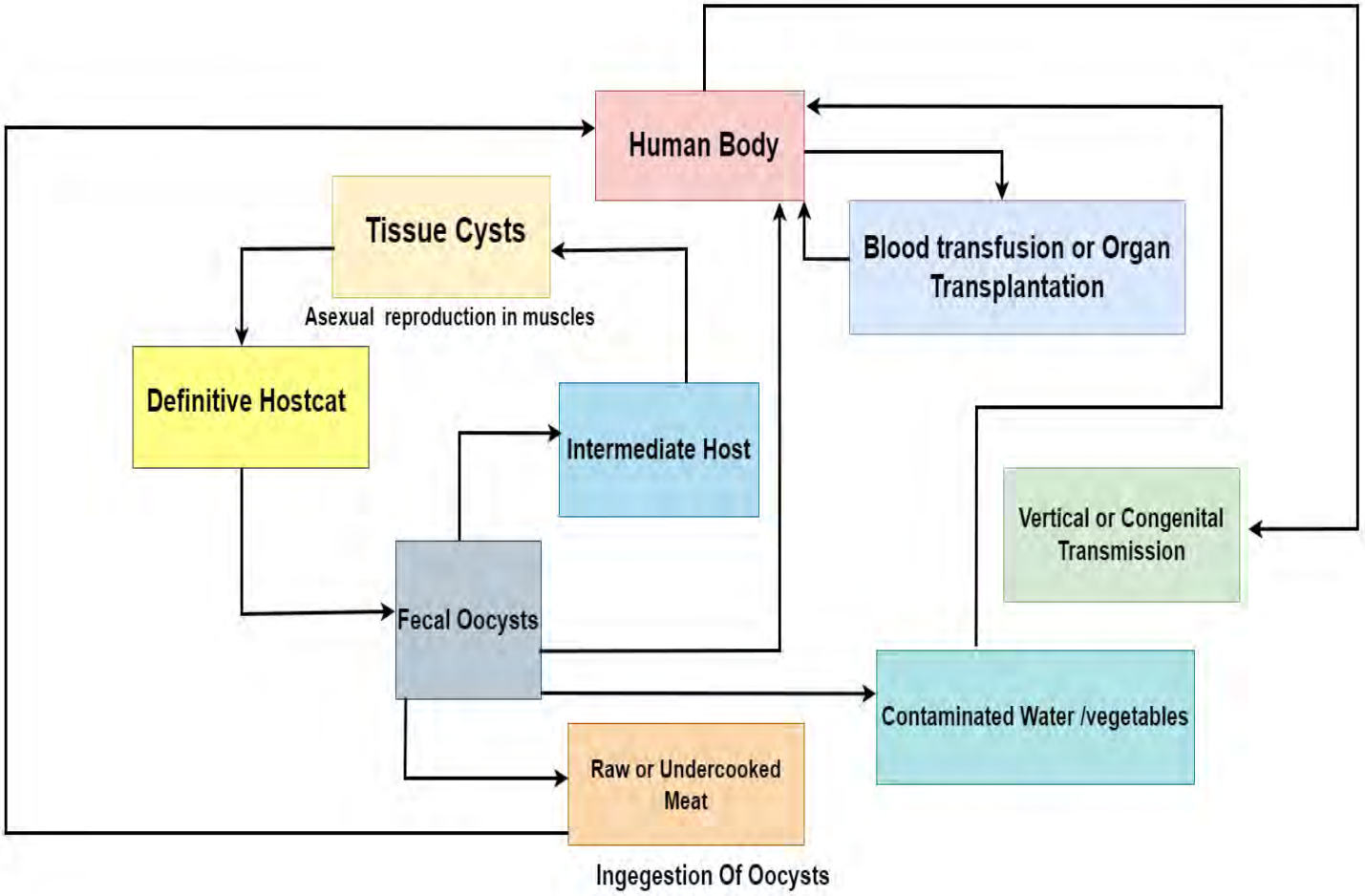

Figure 2.1: Life Cycle of Ocular Toxoplasmosis

2.3 Convolutional Neural Network(CNN)

CNN is a deep learning-based neural network model, processes data using a grid pattern, or images. It was developed by analyzing how the visual cortex of animals is organized [33], which enables it to distinguish between low-level and high-level feature patterns. Convolutional neural networks (CNNs) constructed with three

layers: pooling, convolution, and fully connected layers. Convolution and pooling layer's job is to extract features, and it can be repeated a number of times to extract more features. The fully connected layers get the extracted features so they can map them onto the output for tasks like categorization. The outputs of CNN get progressively more sophisticated as it adds additional layers. In order to improve the outputs' consistency with the "ground truth" labels, the model is trained using a variety of optimisation algorithms, such as back propagation, gradient descent etc.

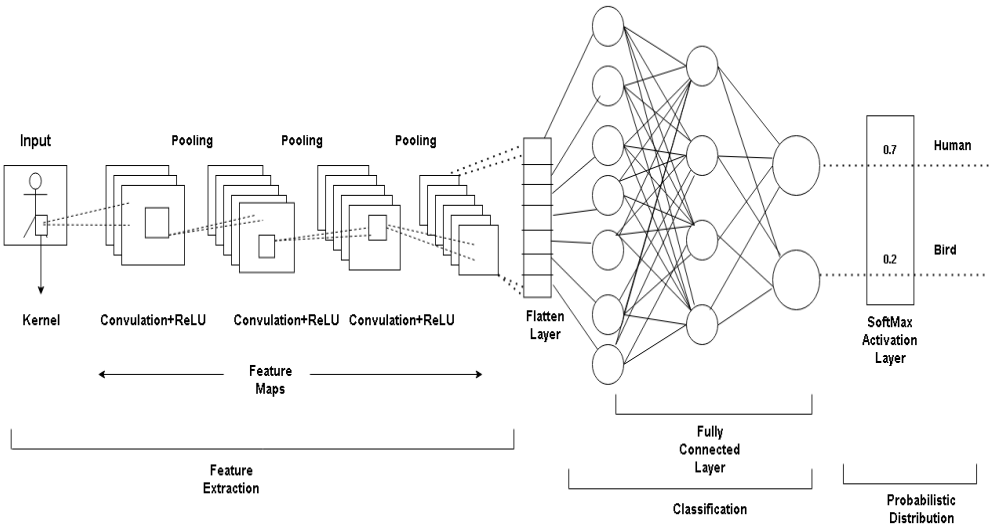

Figure 2.2: Convolutional Neural Network Architecture

2.4 Building Block of CNN Architecture

Several convolutional and pooling layers joined to fully connected layers make up a standard CNN. A typical design often consists of one or more fully linked layers that are followed by repetitions of numerous convolution layers and pooling layers. Forward propagation is the process of transforming input data into output.

2.4.1 Convolution Layer

The convolution layer is crucial in the extraction of features utilising linear and nonlinear mathematical operations like convolution operation and activation.
Convolution is a mathematical operation that includes joining two functions to produce a third function. Two sets of data are combined. The tensor input data is processed using CNN using a small array of integers known as a kernel or filter. The kernel and also tensor components are combined to form an element-wise outcomes that is specific to each spot of the tensor, resulting in a feature map made up of outputs with discrete places in the output tensor. A number of various extra kernels are applied to the input tensor in order to extract different features from the data sets.

Size and number of kernels are the convolution operation's two primary arguments. The most typical kernel size is 33, but 55 and 77 are also frequent. Conventionally, convolutional methods do not permit the kernel's centre to overflow the input tensor's outermost element, which results in a loss of data in the feature map. This problem can be solved by using a method known as zero padding [13] A stride is typically one and is defined as the distance between two successive kernel positions. A larger one is occasionally used to downscale the feature maps. Weight sharing, which describes how the kernels are distributed among different picture locations, is a crucial component of the convolutional procedure. Having the ability for other kernels to use the local features found by one kernel as variables avoids the need to repeatedly identify local features.
Downsampling and a pooling operation can produce a larger feature map and allow for the learning of spatial hierarchies of feature patterns. Additionally, by lowering the number of necessary parameters, the model's effectiveness can be improved

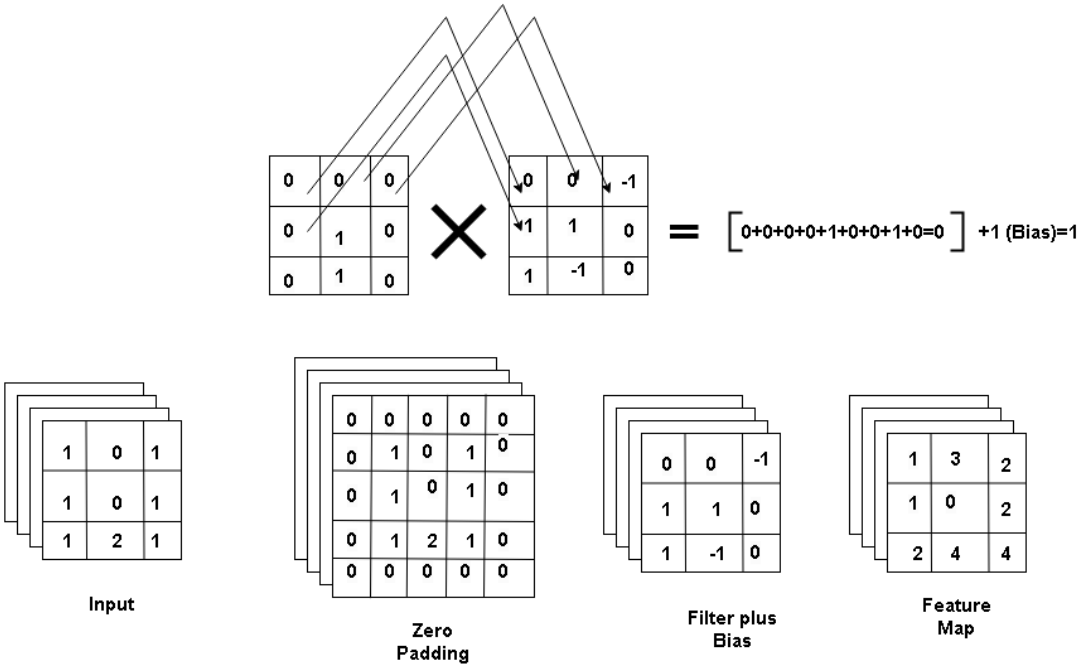

Figure 2.3: Convolution Layer

Convulation operation,C(i,j)-

$$C(i,j) = (Y * W)(i,j) = \sum_{m} \sum_{n} I(m,n) \cdot K(i-m, j-n) \tag{2.1}$$

2.4.2 Non-Linear Activation Function

In artificial neural networks, nonlinear activation functions are extremely important [34] because they are responsible for adding nonlinearity into the model underlying the network. Neural networks are able to recognise intricate patterns and relationships in data because of this nonlinearity. The ReLU is the most common approach in this field.
The formula Sigmoid Activation Function:

$$\sigma(x) = \frac{1}{1 + e^{-x}} \tag{2.2}$$

Formerly utilised in neural networks' hidden layers, but less frequently used now because of problems with vanishing gradients.

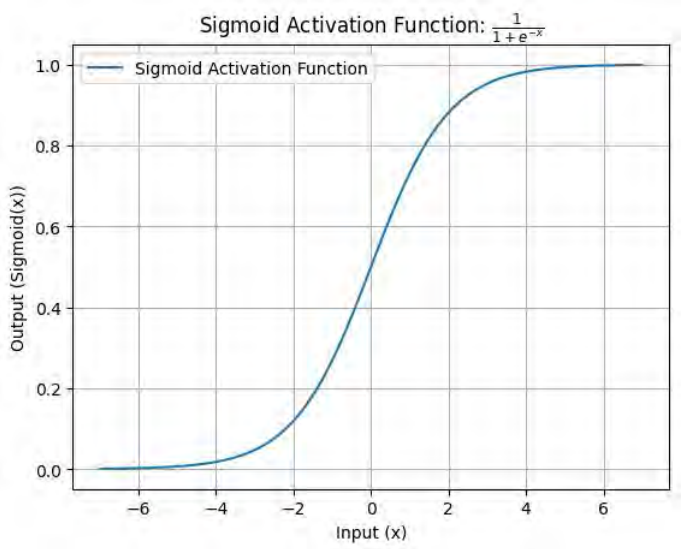

Figure 2.4: Sigmoid Function

The formula of hyperbolic tangent function:

$$\tanh(x) = \frac{e^{x} - e^{-x}}{e^{x} + e^{-x}} \tag{2.3}$$

This is somewhat helpful in mitigating the vanishing gradient problem, as it has a wider output range than the sigmoid.

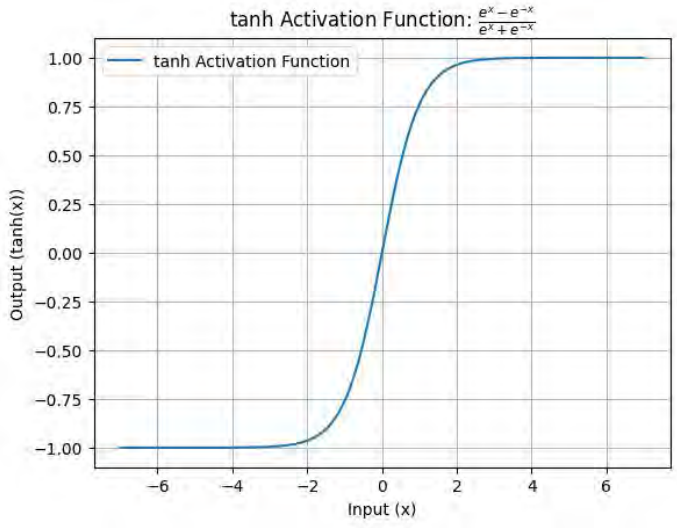

Figure 2.5: Tanh activation function

The formula of Rectified Linear Unit:

$$ReLU(x) = \max(0, x) \tag{2.4}$$

Because of its ease of use and efficiency in training deep neural networks, this activation function is one of the most used ones. On the other hand, it might have the "dying ReLU" issue, in which neurons can stop functioning.

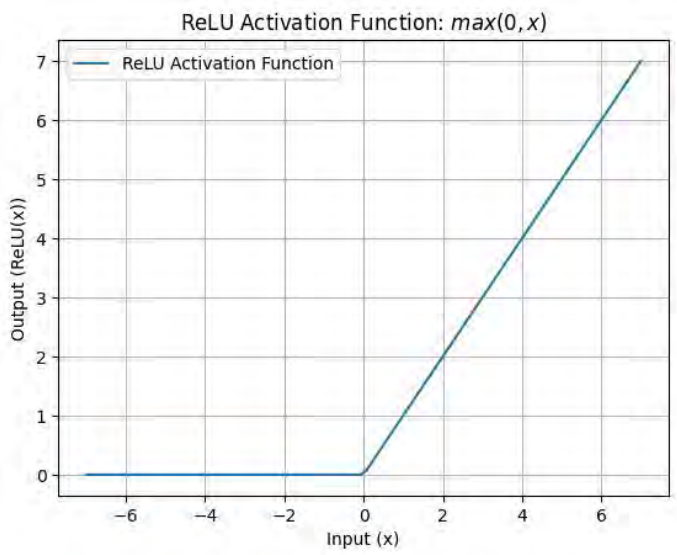

Figure 2.6: ReLU activation function

The formula of Leaky Rectified Linear Unit:

$$LeakyReLU(x) = \max(\alpha x, x) \quad \alpha \text{ is a small positive constant} \tag{2.5}$$

Intended to provide a little, non-zero gradient for negative values in order to alleviate the dying ReLU issue.

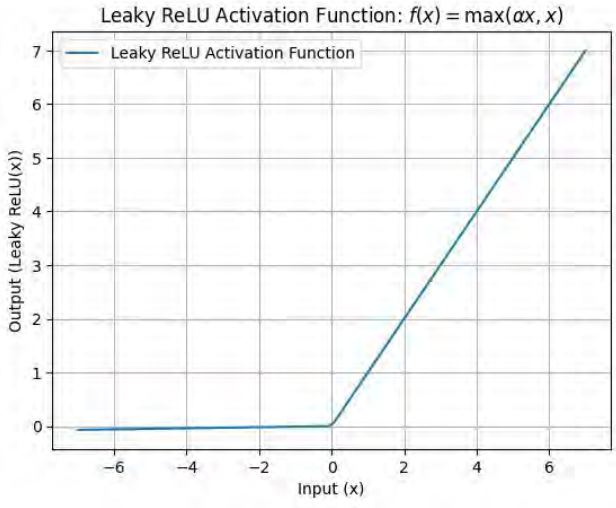

Figure 2.7: Leaky ReLU activation function

2.4.3 Pooling Layer and Max Pooling

The pooling layer is used to lower the size of the feature map in order to produce a translation consistency that can detect minute deviations and distortions and assists in reducing the amount of values learned throughout training. Max pooling, which partitions the feature map into collections of patches, chooses the maximum value for every patch, and ignores the remaining values, is the recommended pooling procedure. The size and stride of the most popular max pooling filter are 2 and 2, respectively.[30].

2.4.4 Fully Connected Layer

One or more fully connected layers, in which every input is coupled to every output by a learn able weight, are connected to the outputs of the convolutional and pooling layers. After the convolution layer has extracted the features and the pooling layer has down sampled them, the features are then passed on to fully connected layers, which generate the final outputs, such as classification probabilities, etc. The final fully linked layer's output nodes are determined by the number of classes. A nonlinear function, such as ReLU, as previously mentioned, follows each layer.

2.4.5 Loss Function

The difference between the actual output and the network output is employed by the loss function to determine the cost via forward propagation. The most popular loss function for multi class classification is cross-entropy, while regression to continuous values typically makes use of mean squared error. In this investigation, the binary cross entropy was used.
The cross-entropy loss for binary classification is given by:

$$\text{LogLoss} = -\frac{1}{N}\sum_{i=1}^{N}[y_i \cdot \log(\hat{y}_i) + (1 - y_i) \cdot \log(1 - \hat{y}_i)] \tag{2.6}$$

2.4.6 Gradient Descent

Gradient descent is an approach to optimisation that constantly modifies the network's learn able parameters, such as kernels and weights, with the main objective of minimizing loss. However, the approach used in this research is called the Adaptive Moment Task Last Layer Activation Function. Binary classification Single-class Multi class Sigmoid [13] Classification Softmax Various classes are classified The Sigmoid Regression to Continuous Values Identity 11 Estimation (Adam) method represents a more significant improvement than the general gradient descent method.

2.4.7 Adam Optimizer

Adam is an adaptive learning rate optimization algorithm that has been compared to a hybrid of the optimization methods root mean square propagation (RMSprop) and stochastic gradient descent (SGD). This is due to the fact that it actually squares

gradients similarly to RMSprop and modifies the learning rate by using the gradient's moving mean instead of its SGD with momentum counterpart [13].Various factors lead to various learning rates because of the method's adaptability. Adam additionally retains the exponentially decaying average of the previous gradients. The typical values for 1 and 2 are 0.9 and 0.999 respectively [25].

2.4.8 Data and Ground Truth Labels

The most crucial components in every machine learning algorithm, including deep learning, are the data sets and the ground truth labels. In actuality, the data set and ground truth label of any such method and models determine their success. Because of this, it is imperative to carefully choose the data sets and ground truth labels, but doing so is costly and time-consuming. There are several widely available, high-quality sources for medical photos. However, the model requires data sets with specified ground truth labels in order to be used for a certain topic or function; as a result, more care must be given.Data sets typically fall into one of three categories: training, validation, or test. As the name implies, the network is trained using a training set, and learn able parameters are updated back into the network via back propagation while loss values are determined by forward propagation. Throughout the entire training process, the validation set is utilized for fine-tuning the hyper parameters and performing model selection. The completed model or network is tested on the test set, and its performance is assessed after being fine-tuned using training and assessment data sets. It is noteworthy that test and assessment sets are maintained separate.

2.5 Over-fitting

Because of over-fitting, the signal in a model has been replaced by statistical regularities specific to the training set when it performs badly on a fresh data set. In other words, rather than learning the signal, it learns the noise or supplementary data that is specific to the data set. Even if there are effective ways to limit overfitting, having more training data is unquestionably the best strategy. There are alternative methods available because this is not always feasible, including regularization with dropout, weight decay, data augmentation, etc.Dropout is a regularization method that reduces the model's sensitivity to certain network weights by randomly choosing some activation's during training and setting them to 0. The "dropout" regularization method involves choosing a number of activation's at random.The regularization method known as "dropout" comprises changing a number of randomly selected activation's to 0 during training.

2.6 Transfer Learning

Despite the fact that large data sets are ideal for model training, they are hard to come by. One way to solve this problem is to use transfer learning, which first trains the network model on a huge data set like ImageNet before reusing it for the target topic of interest. The essential idea is that features can be learned from a large data set and then shared amongst data sets that initially appear to be completely

unrelated. Due to its ability to alter the generic features that have been learned from data sets, deep learning has the advantage of functioning effectively with small data sets in a range of domain tasks. models like AlexNet, VGG, ResNet, and others are examples of this [25].Although there are numerous uses for pre-trained networks, static extraction of features will be the main emphasis of this research. To keep the residual network—which is composed of a series of layers for pooling and convolution called the convolutional base and used as a fixed feature extractor—fully linked layers from a neural network that has been trained in an extensive database must be removed. The new classifier can only be trained on a selected data set of interest by adding fully linked CNN layers to the static feature extractor.

2.7 Deep Learning and it's use in Ocular Toxoplasmosis

Artificial neural networks are used in deep learning, a kind of machine learning, to model and identify patterns in large amounts of complex data. It has multiple uses in many different industries, including healthcare. Deep learning has the potential to significantly affect various aspects of ocular toxoplasmosis.

1. **Diagnosis and Detection:** In order to identify symptoms of ocular toxoplasmosis, deep learning algorithms can be trained to examine medical images like fundus photos, OCT scans, or retinal imaging. These algorithms can be trained to recognize particular disease-related patterns and lesions, assisting ophthalmologists in making precise and timely diagnosis.

2. **Prognosis and Disease Progression:** Deep learning algorithms are able to forecast the course and prognosis of the disease by examining longitudinal data from individuals with ocular toxoplasmosis. These models can use a number of patient-specific variables and data from medical imaging to offer individualized insights on the progression of the disease.

3. **Drug Development and Treatment Planning:** To help in the identification of drugs for the treatment of ocular toxoplasmosis, deep learning can be used to analyze huge data sets, including molecular data and drug-target interactions. Deep learning models can also help with treatment plan optimisation and therapy response prediction based on patient characteristics.

4. **Risk Assessment:** Deep learning algorithms can be applied to determine how likely a community or individual is to contract ocular toxoplasmosis. These models can assist in identifying those who are more likely to contract the disease by taking into account a variety of risk factors, including age, immunological state, and geographic location.

5. **Public Health Surveillance:** Deep learning algorithms can be used to analyze data from a range of sources, including public health databases and electronic medical records, to track the prevalence and spread of ocular toxoplasmosis in different regions. Health authorities may utilize this to support the implementation of targeted interventions and control measures.

Chapter 3

Literature Review

Park et al.shows that ocular toxoplasmosis is a condition brought on by either congenital or acquired infection with Toxoplasma gondii[11].Once inside the retina, the parasite multiplies before rupturing host cells and invading neighboring cells to produce primary lesions. Sometimes the confined parasite can be activated by the host defenses in the primary scar, infecting a nearby lesion. The host immunity in the initial scar can occasionally activate the confined parasite, causing it to infect an adjacent lesion. The main symptom of ocular toxoplasmosis patients is blurred vision, which can be identified by looking for antibodies or parasite DNA. If untreated, ocular toxoplasmosis can sometimes result in vision loss 1 since it requires treatment with numerous drug combinations to get rid of the parasite and the accompanying inflammation.As a zoonotic pathogen, Toxoplasma gondii is a common, obligate intracellular parasite that affects both humans and warm-blooded animals. T. gondii 23 is thought to infect almost one-third of all people on the planet on a chronic basis. The prevalence of the illness and the causes of infection, however, varied between geographical areas with various toxoplasmic settings, such as climatic conditions, dietary customs, and cleanliness standards. Toxoplasmic retinochoroiditis, which accounts for 30-55.

The use of residuals Neural networks (ResNets) for the automatic diagnosis of ocular toxoplasmosis (OT) from fundus images is covered by Parra et al. [22]. The authors emphasize the potential uses of ResNets in ophthalmology and give an outline of the present state of research in this area. They also talk about the difficulties in using ResNets to diagnose OT, and they make suggestions for future studies. The authors next give a thorough review of recent findings in this area, emphasizing ResNets' potential for use in OT diagnosis. They go over how to segment OT lesions using ResNets and how to categorize fundus images into normal and pathological categories. They also go through how ResNets may be used to identify OT lesions in fundus pictures. Finally, the authors talk about the difficulties in applying ResNets to OT diagnosis. They emphasize the significance of huge data sets and high-quality data for machine learning research. A data set of samples is used to fine-tune a pretrained residual neural network. The results demonstrate that the suggested model is quite promising, with sensitivity and specificity rates of 94% and 93% respectively.

M. S. Khan et al.in this study have tried to put up an innovative method to tackle the issue of significantly imbalanced data in the classification of eye diseases[27]. Instead of addressing the initial multi-class classification problem, the researchers

opted to convert it into a series of binary classification tasks, utilizing data-sets that were balanced in terms of class distribution. The execution of this strategic maneuver facilitated the deep learning model, particularly VGG-19, in obtaining an impressive level of accuracy when discerning between typical eye conditions and specific ailments such as myopia, cataract, and glaucoma. The implementation of this strategy intended to address the root cause of class imbalance had a significant role in the achievement of positive outcomes for their automated ocular disease detection system. This study has some problems, such as the possibility of an imbalance in the data,its limited effectiveness to other diseases and data-sets, its reliance on data quality, the lack of clinical validation, the challenges of understanding the model's decisions, ethical concerns, and the need for more research and enhancement in areas like ocular image segmentation and class imbalance handling using generative adversarial networks (GANs).

Computer-aided diagnostic (CAD) systems have started on an exciting new path in the effort to protect eye health. This paper introduces a multi-label convolutional neural network (ML-CNN) system based on multi-label classification (MLC) that is capable of simultaneously detecting a multitude of ocular diseases from color fundus images, a significant advancement over existing systems which tend to focus on individual ocular diseases.Here the researchers(E. AbdelMaksoud)innovated the three pillars of pre-processing,modeling and prediction [29].Their ML-CNN displays exceptional performance, achieving 94.3 percent accuracy, 91.5 percent precision, and 96.7 percent AUC with the help of its three convolution layers, max pooling, dropout layers, and fully linked layers. Beyond its technological prowess, this study stands out for its optimistic outlook on a future where a large, balanced ML data set, com- bined with meticulous manual splitting, promises to further improve diagnostic accuracy and eliminate over-fitting, opening exciting avenues for future research in the field of ocular health.

Using Deep Learning (DL) models, authors Rodrigo Parra, Verena Ojeda, and their team approach the problem of establishing trust in ocular toxoplasmosis (OT) diagnoses[21]. The authors present an unusual method for evaluating the trustworthiness of DL models by comparing their decision criteria to those of ophthalmologists. Their results demonstrate the importance of trust in model selection alongside more conventional measures, especially for medical applications. To further the adoption of DL in the medical community, potential future enhancements include validation by ophthalmologists, alternate attribution approaches, and comparisons with traditional ML models.

M. et al. proposed employing a deep learning algorithm to differentiate between ocular toxoplasmosis (OT) lesions and normal fundus photographs[19]. They collected fundus images of eyes with OT lesions from multiple uveitis facilities, annotated the images, performed patch-level classifications, and then generated a probability heat map using a sliding window protocol. They created a dual-input hybrid CNN model for detecting OT fundus images by integrating the heat map and patch features. Using metrics such as AUC, sensitivity, and specificity, the results showed that the model could be a useful diagnostic aid for ocular toxoplasmosis for clinicians.

In this scholarly work, M. Akil et al. addresses the significant difficulty of detecting ocular pathology from fundus images in the healthcare industry [16]. The

complexity arises from the varying severity phases of pathologies, which can be identified by lesions with distinctive morphological characteristics. In addition, distinct pathologies may exhibit similar characteristics, and patients may be afflicted by multiple pathologies simultaneously. The process involves a complex multi-class classification strategy.The author underlines that methods based on deep learning outperform other approaches due to their ability to adapt network configurations to specific detection objectives. The study investigates these deep learning-based ocular pathology detection methods comprehensively, with a focus on lesion segmentation and pathology classification. The research explores the processing stages, neural network structures, hardware and software requirements, and experimental design principles for method evaluation.Nevertheless, the work identifies several challenges and variations within the field. Even among methods with similar objectives, there is substantial variation in processing techniques, network architectures, input data management, and performance evaluation techniques. The clinical context requires the simultaneous detection of multiple diseases during screening, which represents an immense task for the majority of deep learning-based methods.

Medina et al. show that UWF imaging is a powerful tool for detecting and monitoring retinal illnesses, with the potential to improve clinical evaluation quality and broaden the use of tele ophthalmology in providing efficient eye care [28].The author compares UWF fundus photography to traditional ophthalmoscopy for diagnosing and classifying various retinal disorders.The results showed that graders had high agreement in categorizing retinal disorders using both UWF imaging and ophthalmoscopy. Apart from that, inter-rater agreement was nearly flawless, demonstrating that UWF imaging is a trustworthy alternative to ophthalmoscopy for identifying severe retinal disorders.UWF imaging offers benefits like accurate diagnosis, monitoring of retinal conditions, detailed assessments without discomfort, and validation for teleophthalmology applications, directing patients to appropriate clinical care pathways.

The incorporation of Retina Image Analysis by Jamal A et al revolutionizes in the field of ophthalmology, allowing optometrists to increase their diagnostic capabilities and improve patient care, notably in non-invasive diagnosis and treatment planning [14]. RIA is intended to aid in the study of retinal pictures, with a special emphasis on vascular discovery within the retina. This study's main objective was to give optometrists a powerful tool for examining retinal pictures through the use of an advance interface that offers a variety of options for image processing, analysis, and storage.The discovered vessels are displayed on the retinal picture by RIA for further investigation.Detecting irregularities in retinal pictures can lead to timely actions that could save a patient's sight.RIA improves diagnostic accuracy while decreasing the chance of misdiagnosis.RIA provides valuable insights into retina condition, aiding in better treatment planning and serving educational purposes, though it does not prescribe treatment or medication.

The study [23] suggests an automated screening technique for eye illnesses utilizing fundus images that is based on deep learning. An automated screening technique for agerelated macular degeneration (AMD), glaucoma, diabetic retinopathy (DR), and a few other diseases is presented in this work.The system has a high Cohen's kappa score of 97.6 and a multiple disease classification accuracy of 97%.

Anneke Annassia Putri Siswadi presents CAD models for detecting ocular abnormalities from single-color fundus photography [32]. The first model focuses on detecting microaneurysms with high sensitivity and low number of FPI. The main challenge in MAs detection is the limited number of data with MA, causing severe data imbalance. The MAs detection consists of three main processes: pre-processing, MAs candidate extraction, and MAs classification. The MAs classifiers are built using ensemble and cascade learning methods. The firstmodel uses the enhanced-green channel, background suppression image, and blue channel for MAs detection, while the second classifier uses cascade learning to reduce FPI with high sensitivity. The second model identifies 28 ocular abnormalities, including frequent and rare ones.The model adds a co-occurrence dependency factor, using linguistic features of labels as a semantic dictionary. Two approaches for multi-label detection with deep learning are proposed:CNN-based and Transformer-based semantic dictionary learning. The transformer-based approach achieves higher performance compared to CNN-based semantic dictionary learning.

The author Chakravarthy et al. of this paper focused on A contagious illness called ocular toxoplasmosis brought on by the parasite Toxoplasma gondii, which eats away at good retinal cells[15]. OT diagnosis is a difficult process. Our method involves first developing a network to identify unwell and well-picture portions extracted from a fundus picture.The Next level involves creating a duplex input hybridized system that can take photos and the related fundus photos using the VGG16 architecture programmed on the ImageNet records. For evaluation purposes, the model was programed for hundred epochs for each of the three sample ratios specified in the patch phase CNN.For the testing ratio of seventy/thirty, their model obtained an AUC of (0.949).When the hybridized approach total results are taken into account the (seventy/thirty) sampling ratio outperformed and (fifty/fifty) and (thirty/seventy) in each of the assessment criteria.

In this study, The author Abeyrathna et al.concentrate on the segmentation of fundus pictures with ocular scars and lesions brought on by OT, as well as the detection of all OT scars and lesions, as well as their exact boundaries [18].They first constructed a cutting-edge instance classification network based on Mask R-CNN for dividing OT lesions in corneal fundus photos. Second, they create a novel unsupervised learning-based methodology for expert led studies of ground truth labels for instance segmentation network optimization. The proposed method uses a pre- trained CNN to extract features from the ground truth. K-means clustering is then applied to the feature space to construct tiny clusters of predicted and real-world instances with related characteristics.We demonstrate that this strategy can enhance segmentation effectiveness by evaluating just thirty three percent misclassified examples and then build strategies for optimizing the networks on the basis of professional's suggestion on the misclassified occurrences. Additionally, studying sixty-six percent of those cases yields the similar progress as studying hundred percent of them, demonstrating a thirty four percent decrease in manual labor without sacrificing productivity.

Alam et al.researched Ocular toxoplasmosis (OT) which is a very well known eye disease brought on by T. gondi that can impair eyesight, has not received much attention in research the authors have developed a benchmark research that assesses the performance of current established networks employing transfer learning approaches

to identify OT from fundus fundus photos in order to address this issue[31]. The effectiveness of transfer-learning based segmentation networks for segmenting infections in the photos has also been studied, and in-depth analyses of various feature extraction techniques have been carried out to determine the best technique for OT division and categorization of lesions. We have tested previously trained methods including (VGG16, MobileNetV2, InceptionV3, ResNet50, and DenseNet121) models for classification tasks.MobileNetV2 performed better than all other methods in terms of (Accuracy and Recall, and F1 Score), surpassing InceptionV3 by 0.7% in Acc. However,DenseNet121 outperformed MobileNetV2 in terms of Precision, coming in with a 0.1% advantage, Its work has utilized U-Net architecture for the segmentation task(MobileNetV2 and InceptionV3 and ResNet34, and VGG16) were used to upgrade various structure in order to use transfer learning. When the Jaccard loss function is used during the training,MobileNetV2/UNet outperformed ResNet34 in terms of Acc and Dice Score by 0.5% and 2.1%, respectively.

J. G. Montoya et al.discuss the diagnosis of toxoplasmic retinochoroiditis, highlighting the challenges in detecting a systemic immune response within a localized occurrence [8]. The author's suggested using aqueous humor analysis for specific antibodies or parasitic DNA, but acknowledge the need for vitreous sampling. They also discuss the challenge of laboratory confirmation due to inter-individual variances in antibody production. They propose a tailored diagnostic algorithm for atypical clinical presentations and suggest that laboratorybased tests can improve clinical diagnoses. They also explore the enigmatic aspects of humoral immunity in toxoplasmosis, including the diagnostic window for false-negative results, differences in antibody detection, and the role of non-specific immune stimulators. They emphasize the need for further scholarly endeavors in this area.

J. E. Gomez-Marn et al.conducted a study in Armenia-Quindo, Colom- ´ bia, to investigate the prevalence of retinochoroidal lesions caused by ocular toxoplasmosis and their association to risk factors [20]. The researchers evaluated 161 people and discovered that 10.5% of them had retinochoroidal scars, indicating an old dormant Toxoplasma gondii infection. All 17 patients with these lesions tested positive for T. gondii antibodies. Bottled water intake was found to be a protective factor against T. gondii infection in this community. Despite such limitations, the study discovered a statistically significant protective factor in bottled water use. The risk factor assessment was based on patient interviews, which could create recall bias.To address this, a standardized questionnaire was utilized. The study emphasizes the significance of toxoplasmosis-related ocular lesions in Armenia-Quindo, Colombia, and advocates for promoting the consumption of boiled or bottled water as a significant preventive public health measure to reduce T. gondii infection and the subsequent onset of ocular toxoplasmosis.

Clinical Manifestations of Ocular Toxoplasmosis" by Delair et al. discuss the signs and treatments for ocular toxoplasmosis [7]. The disease is caused by an infection with Toxoplasma gondii, either acquired or congenital. Once the parasite enters the retina, it multiplies within the host cells before rupturing them and invading adjacent cells to produce primary lesions. The primary symptom of ocular toxoplasmosis is impaired vision, which can be diagnosed by examining antibodies or parasite DNA. Vision loss may result from untreated ocular toxoplasmosis. Multiple treatment combinations are required to treat the parasite and its associated inflammation.

The three distinct types of T. gondii are tachyzoites, tissue cysts (which contain bradyzoites), and oocysts. In approximately one-third of countries, T. gondii is believed to cause chronic infections in humans. However, the prevalence of the disease and the causes of infection varied between geographic regions with different toxoplasmic conditions, such as climate.

This comprehensive literature review explores the complex nature of ocular toxoplasmosis, focusing on its postnatally acquired form. The researcher (Kalogeropoulos) synthesizes research from the PubMed database and Google Scholar, highlighting its clinical features, diagnostic methodologies, and therapeutic strategies[26]. They suggest that identifying characteristic clinical findings is crucial for identifying the disease, and recommend laboratory confirmation through traditional antibody detection or PCR techniques. The author recommends conventional treatment regimens like oral pyrimethamine, sulfadiazine, and corticosteroids as the mainstay, while acknowledging alternative treatment modalities. The review concludes with a forward-looking perspective, envisioning future research in epidemiology, pathogenesis, diagnosis, and treatment to enhance our understanding of ocular toxoplasmosis and refine its management.

Chapter 4

Methodology

The approach recommended for this thesis is illustrated in this section. The gathering, organization, and application of methods for pre-processing to the database mark the first steps of the workflow.In order to ascertain which model has been most successful in case of identifying and binary categorizing photographs of normal and abnormal eyes, the workflow consists of a standard CNN model and the transfer learning approach of four pre-trained CNN models (VGG16, VGG19, ResNet50, Mobilenet). The effectiveness of each of these models compared to using metrics such as accuracy, precision, recall, F1 score, confusion Matrix, and AUC curve. The workflow for the methodology is shown in full in Figure 4.1 as a block diagram.

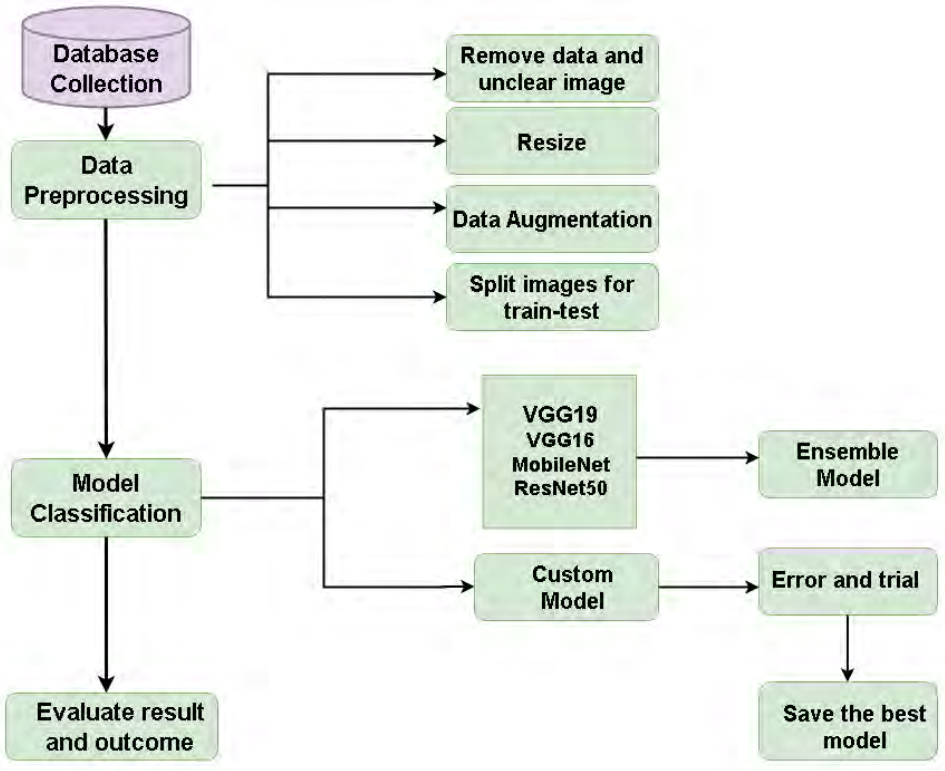

Figure 4.1: Overview of the Proposed Method

4.1 Data Description

Images of the eyes pictures were Collected at the **Hospital de Clnicas medical facility in Asuncion, Paraguay** and **the Niños de Acosta Ñú General Pediatric Hospital** which are part of the Ocular Toxoplasmosis (OT) Fundus Images Data set. According to the fundus photos supplied, the patients may have had a congenital infection of toxoplasmosis. This data set divided into two classes which are healthy and unhealthy. Later on unhealthy class divided into three classes which are active, inactive and active-inactive. We were also able to use this dataset for our research because the authors made it publicly available [35]. A total of 291 colour fundus pictures were obtained at the Hospital de Clínicas' Department of Ophthalmology, Facultad de Ciencias Médicas, Universidad Nacional de Asunción, San Lorenzo 2160, Paraguay. The Niños de Acosta Ñú General Paediatric Hospital utilised the Pictor Plus-Portable Ophthalmic Camera to capture 121 colour fundus images. The data set is used to create models for toxoplasmosis in the eye that may be detected automatically. The fundus images were taken using the Pictor Plus-Portable Ophthalmic Camera and the ZEISS VISUCAM 500 camera.

Table 4.1: Category of Fundus images

Category	**Number of Images**
Healthy	291
Active	68
Inactive	375
Active-Inactive	126
Total	**860**

4.2 Exploratory Data Analysis

Two primary folders comprise the data set one containing all the photos that were gathered and the other including masks for lesions on eyes caused by ocular toxoplasmosis.
This folder contains the original eye images that are being studied. The eye itself, as well as any lesions or abnormalities, are likely to be included in these photos, along with other information. The healthy photographs and non-healthy images are both in the categorization folder. Images showing active, inactive and active inactive lesions carried on by ocular toxoplasmosis can be found in the non-healthy group.

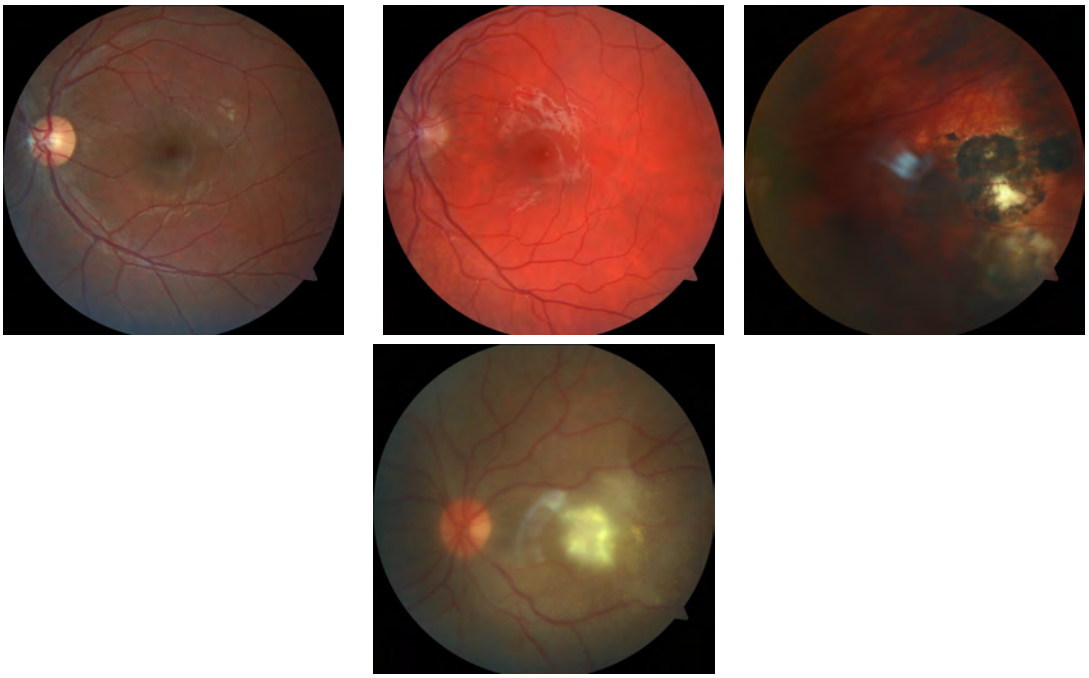

Figure 4.2: Example of Fundus Images from the data set

Mask: This folder contains binary pictures (masks) with labels designating whether each pixel is a part of the lesion or not. A black-and-white map-like representation of the mask indicates which pixels in the associated eye image relate to the lesion or area of interest and which ones do not. Typically, lesions are represented by white (or 1) pixels, while healthy pixels are represented by black (or 0) pixels.

4.2.1 Data Pre-processing

1. **Data Segmentation:** Using Label Studio, a professional ophthalmologist segmented lesions related to toxoplasmosis, both active and inactive. The pictures were loaded and labelled first.The best segmentation was then carried out, and the segmented images' masks were extracted after that. Marking the segments or pixels of the image that include the lesion and stating the type of lesion is the optimum segmentation. The dataset's mask folder contains the obtained masks.

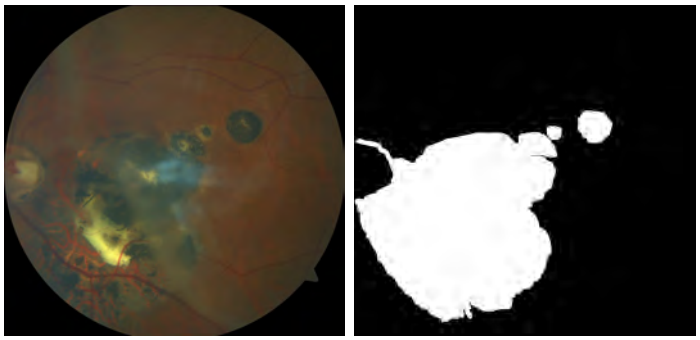

((a)) 113 ((b)) 113_Mask

Figure 4.3: Example of segmentation of the above image with inactive lesion.

2. **Augmentation:** Small data sets pose a significant barrier to research advancement, as neural network models often over-fit and memorize data rather than relationships. Augmentation aims to enhance dataset size, improve diversity, boost model generalization, and handle object orientation variations. Moving from multi-classification to binary classification improves model performance and interpret ability by creating a more balanced data set. This balance can reduce class imbalance problems in multi-class scenarios, preventing biased models. However, class imbalance can result in biased models if the majority class is predicted more often than the minority class.

   Resize Images: Resizing images in image datasets for deep learning is vital to maintain consistency, cut down on computing cost, increase model compatibility, and assure consistent and effective training. That's the reason photos were reduced from their original resolution of pixels to 224x224 pixels proportionately.

   Rotation: The photos were 20 degrees anticlockwise rotated. It makes the adjustments appear minimal.

   Fliping: Images are flipped both hozirontal nad vertical axis.

   Gausian Noise: In order to create Gaussian noise, it is usually done to sample random values from a Gaussian distribution and add them to an image's pixel values.

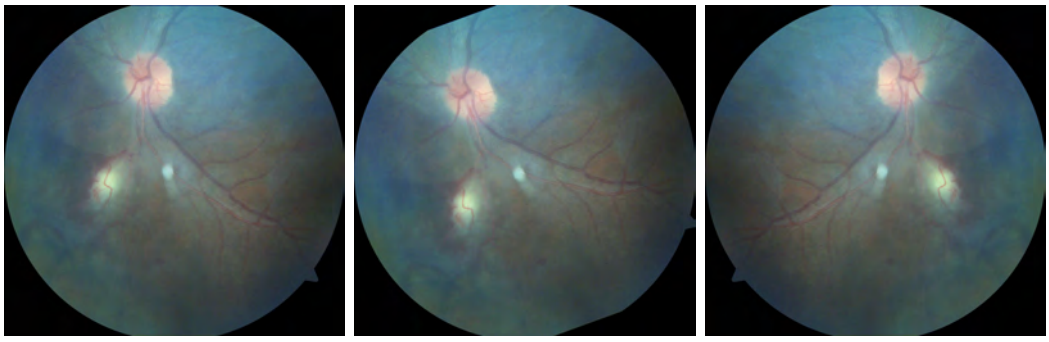

((a)) Orizinal ((b)) Rotate ((c)) Horizontal Flip

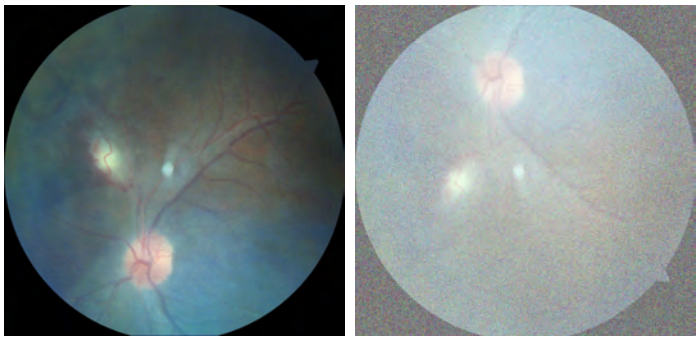

((d)) Vertical Flip ((e)) Gausian Noisy

Figure 4.4: Before and after Augmentation

Augmentation will help to improve the diversity of training dataset, boosts model generalisation, and allows models to deal with variations in object orientation.

3. **Data Splitting:** The study aims to predict if a patient has ocular toxoplasmosis by training and testing a dataset using a split method, which efficiently develops and evaluates deep learning models. It ensures to avoiding overfitting, fine-tuning hyperparameters, and evaluating the model's impact on unseen information to make sure that mode performs well in actual situations. Consequently, the final dataset now included the initial 5200 photos divided into the 2 categories in a ratio of 4000:1200.

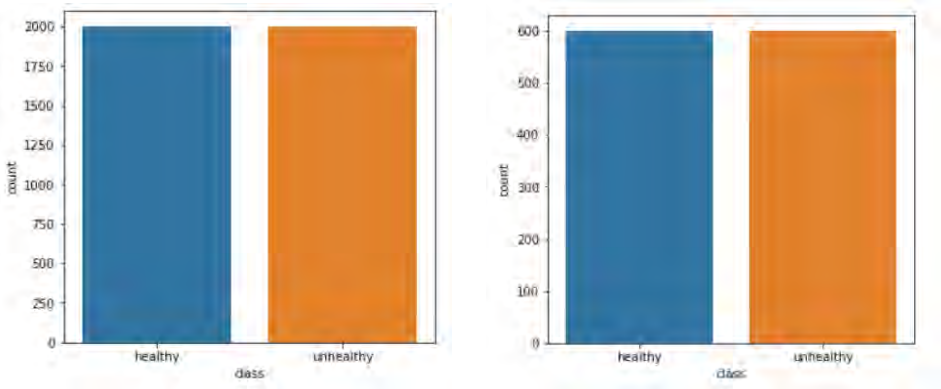

Figure 4.5: Split Between Train and Test

4.3 Model Specification

After finishing the data preparation process detailed in Chapter 4 of that chapter, the dataset may now be put into CNN models to generate a relationship between the image features and the final interpretation. The data set was partitioned once more in a ratio of 75:25 for training, testing respectively.

4.4 Proposed Model

1. **Convolutional 2D Layer:**
    - **1st Conv2D layer:** With a kernel size of (3, 3), the first convolutional layer, conv2D_3, generates 128 feature maps by processing the input images. After batch normalization, which normalizes the inputs of the layer, the ReLU activation function adds non-linearity to the model and improves training stability. 3,584 parameters are added by this layer to the overall model architecture.
    - **2nd Conv2D layer:** Conv2D_4, the second convolutional layer, creates 32 feature maps by using a (3, 3) kernel to further analyze the feature maps produced by the previous layer. ReLU activation and batch normalization are applied, just like in the layer above. There are 36,896 parameters in total for this layer.
    - **3rd Conv2D layer:** Using a (3, 3) kernel, the third convolutional layer, conv2d_5, completes the hierarchical feature extraction process and generates 64 feature maps. Once more, batch normalization and ReLU activation are used, adding 18,496 parameters to the model.

- **4th Conv2D layer:** Lastly, 128 feature maps are produced by the fourth convolutional layer, conv2D_6, using a (3, 3) kernel to process the data. Applying batch normalization and ReLU activation, this layer increases the total number of parameters in the model by 73,856.

2. **Max Pooling Layer:** The Max Pooling layer is used in the model to specially downsample feature maps, reducing dimensional while maintaining relevant data. This enhances the model's ability to identify patterns and features by selecting maximum values within local regions.

3. **Batch Normalization:** Four batch normalization layers are present. We used the Batch Normalization layer following each convolution layer. In 35 epoch, this layer normalizes activation, which speeds up and stabilizes our customized CNN model.

4. **Flatten Layer:** The model's flatten layer flattens 2D feature maps into a 1D vector, facilitating data transfer from convolutional layers to fully connected layers for processing and classification.

5. **Dense Layer:** The model uses three dense layers for feature extraction and transformation, with the first providing a high-dimensional representation, the second providing a compact representation, and the final producing binary classification probabilities.

Table 4.2: Number of Parameters in Proposed model

Layer (type)	**Output Shape**	**parameters**
conv2D_3 (Conv2D)	(None, 126, 126, 128)	3584
max_pooling2D_3 (MaxPooling2D)	(None, 63, 63, 128)	0
batch_normalization_3 (Batch Normalization)	(None, 63, 63, 128)	512
conv2D_4 (Conv2D)	(None, 61, 61, 32)	36896
max_pooling2D_4 (MaxPooling2D)	(None, 30, 30, 32)	0
batch_normalization_4 (Batch Normalization)	(None, 30, 30, 32)	128
conv2D_5 (Conv2D)	(None, 28, 28, 64)	18496
max_pooling2D_5 (MaxPooling2D)	(None, 14, 14, 64)	0
batch_normalization_5 (Batch Normalization)	(None, 14, 14, 64)	256
conv2D_6 (Conv2D)	(None, 12, 12, 128)	73856
max_pooling2D_6 (MaxPooling2D)	(None, 6, 6, 128)	0
batch_normalization_6 (Batch Normalization)	(None, 6, 6, 128)	512
flatten (Flatten)	(None, 4608)	0
dense (Dense)	(None, 256)	1179904
dense_1 (Dense)	(None, 64)	16448
dense_1 (Dense)	(None, 2)	130

Proposed CNN Model Summary: The weights and biases that the network picks up during training are referred to as the number of parameters in a neural network layer. A layer of a neural network receives inputs, processes them using activation functions and matrix multiplication, among other operations, and outputs the results. For the given system, we created a sequential CNN model with the Keras neural network framework. Our customized CNN Model Structure is given above in table 4.2 which will makes the structure more understandable. This model has

in total 16 layers. Six 2D convolutional layers, six max pooling layers, and an equal number of batch normalisation layers were also added. Additionally, one flatten layer and three dense layers were present. This model has a total of 1,330,722 parameters, where 1,330,018 are trainable parameters and 704 are non-trainable parameters.

Here in figure 4.6 we have constructed the model proposed CNN model.

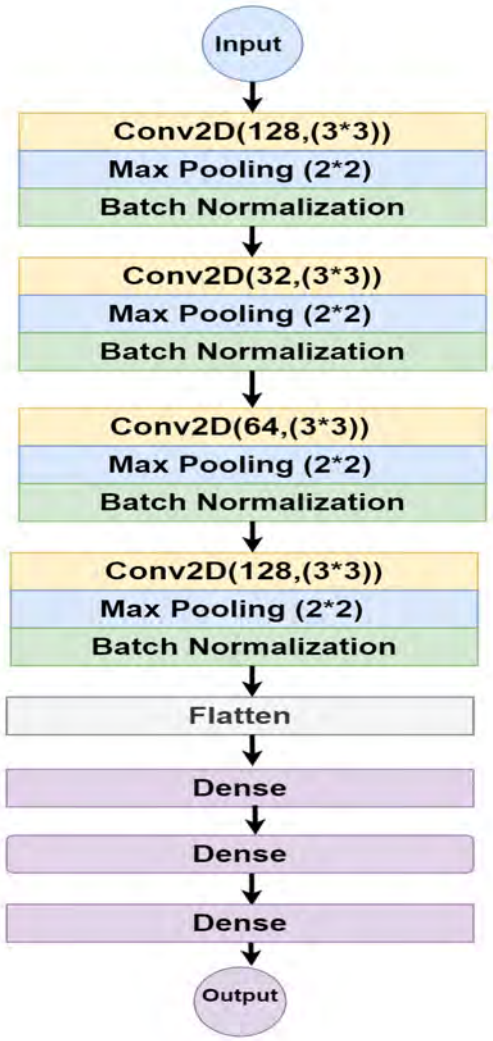

Figure 4.6: Custom CNN Model Architecture

4.4.1 VGG-16:

VGG-16 is a convolutional neural network (CNN) architecture with 16 layers, known for its simplicity and effectiveness in image classification tasks.

1. VGG-16 has 16 layers that can learn lots of details in pictures, helping it understand and recognize different features.
2. It uses 3x3 filters for making its structure simple and easy to follow, helping us understand how it works.
3. VGG-16 was trained on a big dataset called ImageNet, making it smart and ready to be used for recognizing things in new pictures.
4. Whether it's figuring out what's in a picture or finding objects, VGG-16 can handle various jobs because of its balanced design.
5. VGG-16 keeps things simple, making it easier for researchers and users to understand how it makes decisions in different situations.

Here in figure 4.7 we have constructed VGG-16 model.

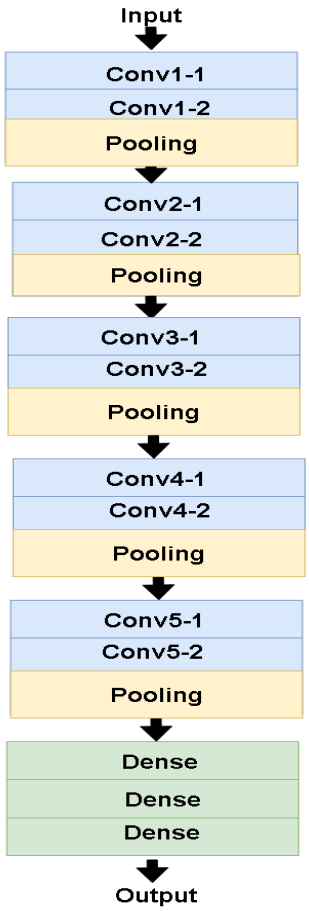

Figure 4.7: VGG16 Model Architecture

4.4.2 VGG-19:

1. A well-known architecture called VGG-19 is renowned for its efficiency in picture classification tasks.
2. Due to its simple design and simplicity, it acts as a great baseline for a variety of computer vision applications.
3. Transfer learning can be performed using pre-trained VGG-19 models, which saves time and resources as compared to training on big data sets.
4. Because of its depth and architecture, the VGG-19 allows to suitable for many different image recognition applications.
5. With availability of pre-trained models and implementations, VGG-19 has broad community support, making project adoption easier.

Here in figure 4.8 we have constructed VGG-19 model.

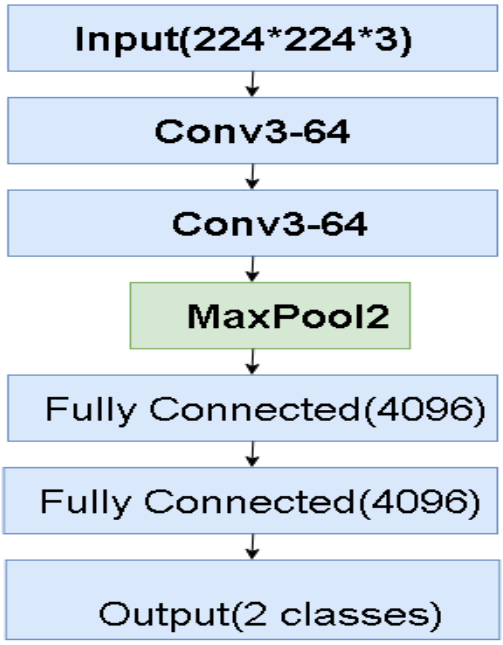

Figure 4.8: VGG-19 Model Architecture

The formula of VGG16 and VGG19 are given below.

Convoluation Layer.

$$H_{\text{out}} = \left\lfloor \frac{H_{\text{in}} + 2P - F}{S} \right\rfloor + 1 \tag{4.1}$$

$$W_{\text{out}} = \left\lfloor \frac{W_{\text{in}} + 2P - F}{S} \right\rfloor + 1 \tag{4.2}$$

Max Pooling Layer.

$$H_{\text{out}} = \left\lfloor \frac{H_{\text{in}} + F}{S} \right\rfloor + 1 \tag{4.3}$$

$$W_{\text{out}} = \left\lfloor \frac{W_{\text{in}} + F}{S} \right\rfloor + 1 \tag{4.4}$$

ReLU activation function:

$$ReLU(x) = max(0, x) \tag{4.5}$$

4.4.3 ResNet-50:

In 2015 it was introduced by He Kaiming and his team. Later on it has became a very widely used architecture for different computer vision.

1. It has 50-layers deep neural network which helps to capture complex hierarchical features in data, making it ideal for high-level feature learning tasks.
2. It introduces a residual connection. It helps to bypass certain layer during training. This feature reduce the vanishing gradient problem.
3. As of now, it is a pretty complex neural network with 50 layers.
4. It's depth and remaining connections help it recognise objects and patterns in images with a high degree of precision.
5. It can pre-trained on large data set like ImageNet. Also can fine tune on smaller data sets for specific tasks and saving time and resources.
6. The ResNet-50 architecture exhibits adaptability and suitability for various computer vision applications, encompassing tasks such as picture classification, object recognition, and segmentation. Additionally, it offers reliable performance and substantial depth for a diverse array of applications.

The equation of ResNet-50 is giver below.

$$H_{\text{out}} = \left\lfloor \frac{H_{\text{in}} + 2P - F_{\text{conv1}}}{S_{\text{conv1}}} \right\rfloor + 1 \tag{4.6}$$

$$W_{\text{out}} = \left\lfloor \frac{W_{\text{in}} + 2P - F_{\text{conv1}}}{S_{\text{conv1}}} \right\rfloor + 1 \tag{4.7}$$

Pooling Layer:

$$Input = H\text{in} * W\text{in} * D\text{in} \tag{4.8}$$

$$Output = 1 * 1 * D\text{in} \tag{4.9}$$

Here in figure 4.9 we have constructed ResNet-50 model.

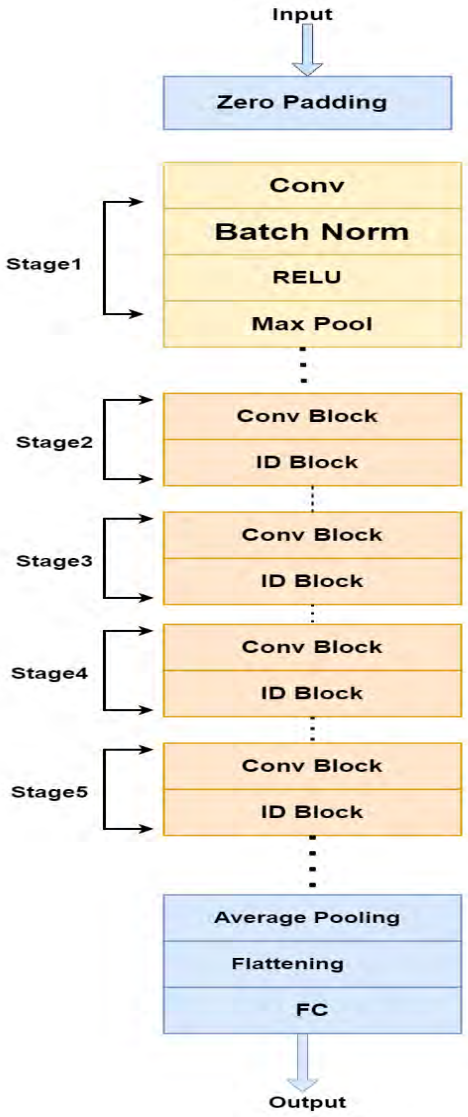

Figure 4.9: ResNet-50 Model Architecture

4.4.4 MobileNetV3:

This model was introduced by Google and it is famous for its light weight and efficient design.

1. MobileNetV3 models are ideal for deployment on mobile devices, embedded systems, and edge devices because of their exceptional resource and memory efficiency.

2. It reduces complexity. So it can run faster in larger data set and making them ideal for real-time application.

3. It has low inference latency which is crucial for applications where quick response times are required.

4. MobileNetV3 is highly suited for mobile applications and settings with limited resources because it helps preserve battery life and lowers data usage.

Equation of MobilenetV3 is given below.
DepthWise Separable convolution:

$$H_{\text{out}} = \left\lfloor \frac{H_{\text{in}} + 2P_{\text{dw}} - F_{\text{conv1}}}{S_{\text{conv1}}} \right\rfloor + 1 \tag{4.10}$$

$$W_{\text{out}} = \left\lfloor \frac{W_{\text{in}} + 2P_{\text{dw}} - F_{\text{conv1}}}{S_{\text{conv1}}} \right\rfloor + 1 \tag{4.11}$$

Pointwise Convolution:

$$H_{\text{out}} = \left\lfloor \frac{H_{\text{in}} + 2P_{\text{dw}} - 1}{S} \right\rfloor + 1 \tag{4.12}$$

$$W_{\text{out}} = \left\lfloor \frac{W_{\text{in}} + 2P_{\text{dw}} - 1}{S} \right\rfloor + 1 \tag{4.13}$$

Global Average Pooling:

$$Input = H * W * D \tag{4.14}$$

$$Output = 1 * 1 * D \tag{4.15}$$

Here in figure 4.10 we have constructed MobileNetV3 model.

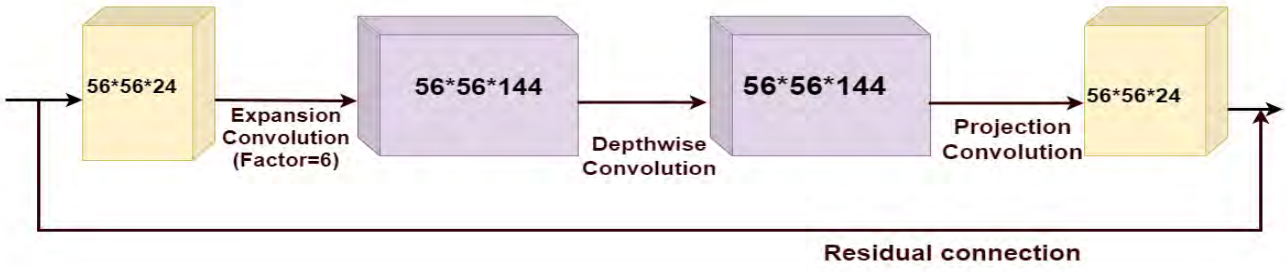

Figure 4.10: MobileNetV3 Model Architecture

4.5 Ensemble Model

1. **Models:**

   VGG16: Building convolutional layers are followed by fully connected layers, and this design is known for its simplicity. Hierarchical features are captured.

   ResNet50: Uses residual connections to lessen the issue of vanishing gradients. Capturing long-range dependencies, appropriate for deep networks.

   MobileNet: Using depth-wise separable convolutions, this efficient design is appropriate for environments with limited resources.

   VGG19: More in-depth and capable of capturing intricate patterns with more convolutional layers than VGG16.

2. **Input:** VGG16 receives the data. Similarly, ResNet50, MobileNet, and VGG19 models also receive the data. Every model has been modified to take in shape-based input (128, 128, 3).

3. **Architecture:** The outputs of the last layers of VGG16, ResNet50, MobileNet, and VGG19 are concatenated following individual training. For the final classification, a fresh set of dense layers is added to the concatenated output. The various features that each base model learns are combined in the ensemble model.

4. **Training Process:**

   Ensemble models improve overall predictive performance by utilizing the diversity of individual models. A wider variety of features and patterns can be captured by combining various architectures. When compared to individual models, it offers a more reliable and generalizable model. Reducing overfitting and enhancing the model's capacity to generalize to new data are two benefits of the ensemble approach. The ensemble model can adjust and fine-tune the combined features for improved performance by being trained over more epochs.

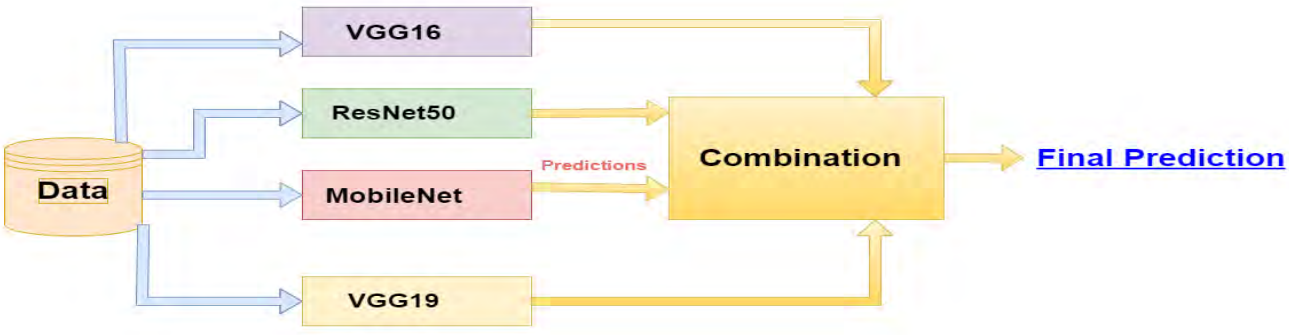

Figure 4.11: Ensemble Model Architecture

Chapter 5

Results and Discussion

5.1 Performance Metrics

Parameters such as accuracy, recall, f1 score, precision, macro average, and weighted average were used to assess the model's performance [17]. Some of the metrics' formulas are given as:
The formula for Precision is given by:

$$\text{Precision} = \frac{\text{True Positive}}{\text{True Positive + False Positive}} \tag{5.1}$$

The formula for Recall is given by:

$$\text{Recall} = \frac{\text{True Positive}}{\text{True Positive + False Negative}} \tag{5.2}$$

The formula for F1 Score is given by:

$$\text{F1 Score} = \frac{2 \times \text{Precision} \times \text{Recall}}{\text{Precision + Recall}} \tag{5.3}$$

The formula for Accuracy is given by:

$$\text{Accuracy} = \frac{\text{Number of correct predictions}}{\text{Total Number of Predictions}} \tag{5.4}$$

5.1.1 Confusion Matrix

A confusion matrix is a table refers to assess how well a categorization system performs.. A confusion matrix visualizes and summarizes the results of a classification algorithm[17] . As a result, there are 4 possible results in a binary classification:
1. **True Positive (TP):** When the results match both expectations and reality, this is a true positive (TP).
2. **True Negative (TN):** when the results are not what was anticipated or what happened as predicted.
3. **False Positive (FP):** Also relied to as a Type 1 error, this mistake type happens when a positive result is anticipated but the actual outcome is negative.
4. **False Negative (FN):** also known as Type 2 error, happens when a result is predicted to be negative but really turns out to be positive.

5.2 Model Evaluations

5.2.1 Performance Study on Custom CNN Model

The Proposed custom model showed significant improvements after 35 epochs of training. It begin the first epoch with a loss of 0.3935 and an accuracy of 83.86%, and it progressively decreased the loss and raised the accuracy. The model achieved a minimal loss of 0.0093 and an accuracy of 95.72% by the 35th epoch, which is noteworthy. The model's strong performance was further demonstrated by its high , recall, and precision values. Improvements were also seen in the validation results, where the model continuously outperformed in terms of precision, recall, accuracy. To further refine the model, learning rate modifications were made, such as a reduction to 1e-05.

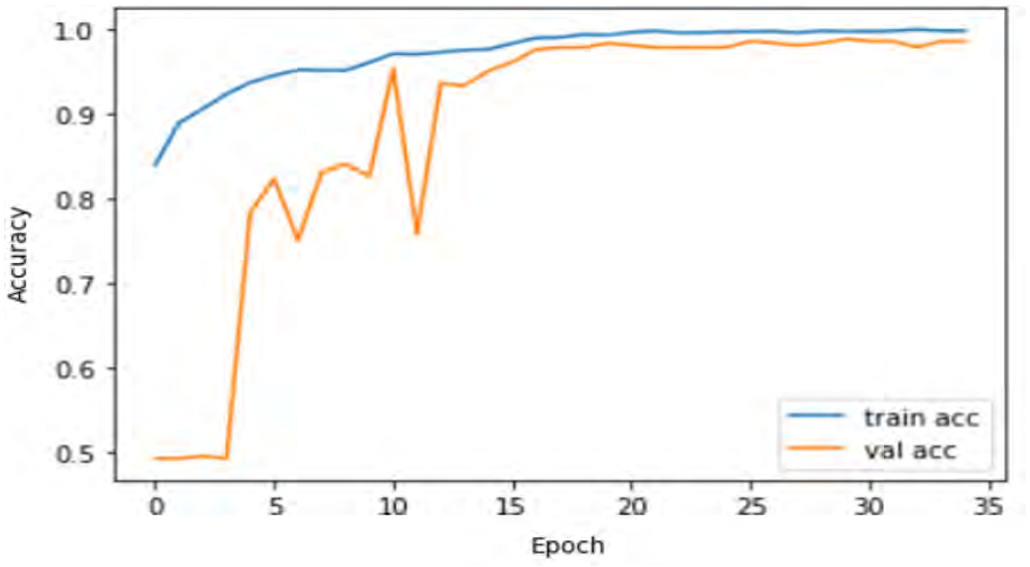

Figure 5.1: Accuracy Graph obtained from applying Custom CNN Model

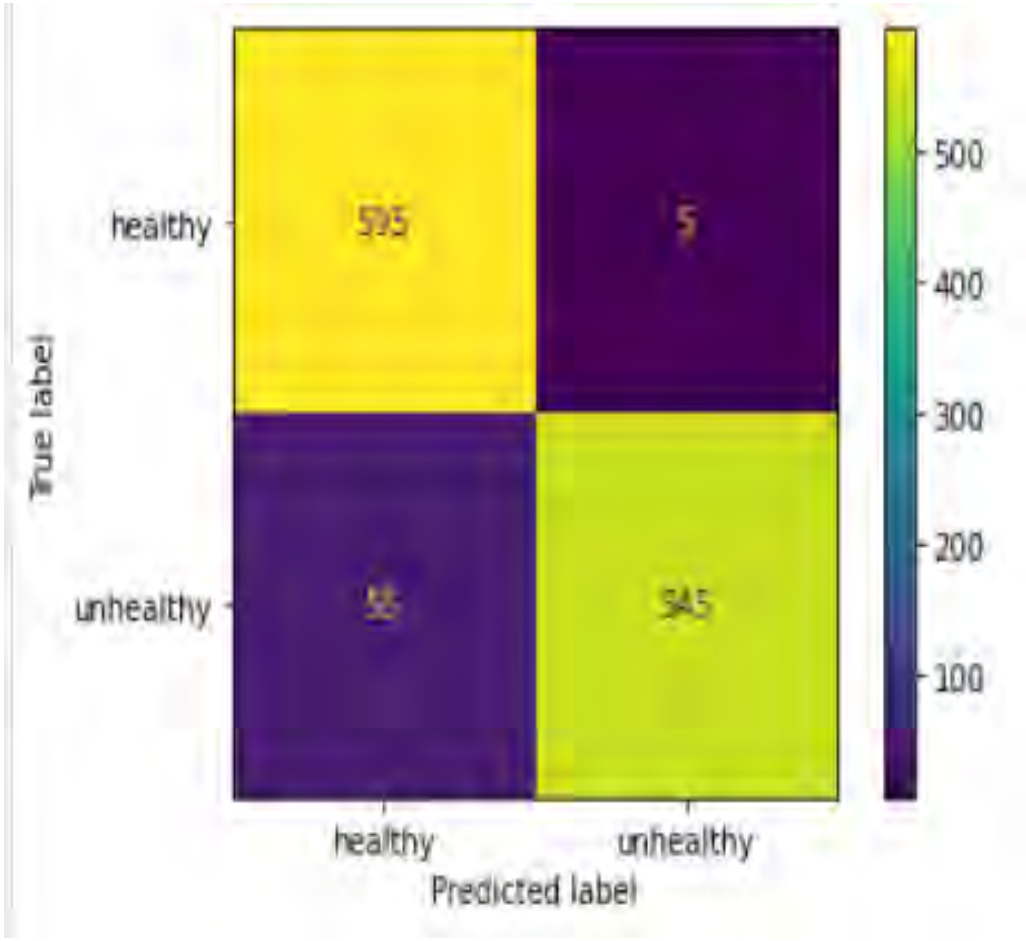

Figure 5.2: Confusion Matrix of Custom CNN Model

Table 5.1: Precision, Recall and f1-score of Custom CNN Model

	precision	**recall**	**f1-score**	**support**
healthy	0.92	0.99	0.95	600
unhealthy	0.99	0.91	0.95	600
accuracy			0.95	1200
macro avg	0.95	0.95	0.95	1200
weighted avg	0.95	0.95	0.95	1200

5.2.2 Performance Study on VGG-16 Model

With a beginning learning rate of 0.001, the VGG-16 model was trained across 35 epochs, tracking metrics such as accuracy, precision, recall and optimizing weights. Over the course of the epochs, the model demonstrated progress in a number of performance indicators on the training and validation sets. Notable results include increased precision, recall and accuracy. Validation loss decreased from 0.3747 to 0.1526, whereas validation accuracy increased from 0.8225 to 0.9350. Adaptively, the learning rate was adjusted throughout training: after the 23rd epoch, it was set to 0.0001, and after the 33rd epoch, it was set to 1e-05.

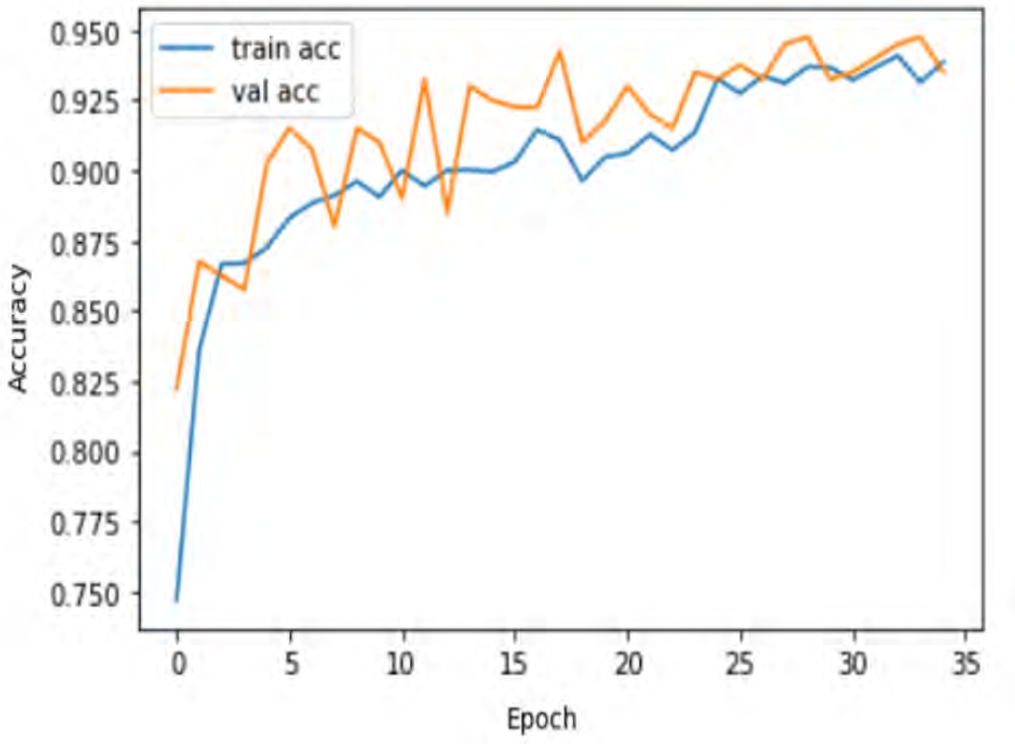

Figure 5.3: Accuracy Graph obtained from applying only VGG-16 Model

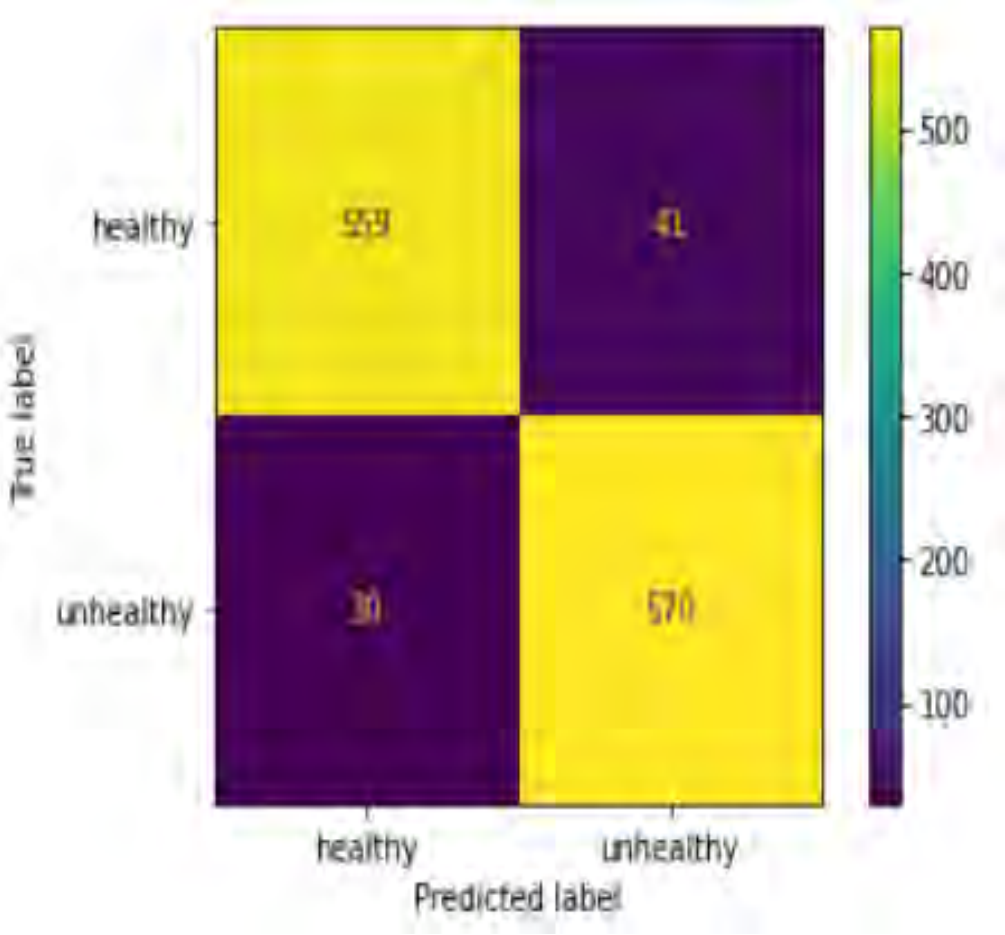

Figure 5.4: Confusion Matrix of VGG-16 Model

Table 5.2: Precision, recall and f1-score of VGG-16 Model

	precision	**recall**	**f1-score**	**support**
healthy	0.95	0.93	0.94	600
unhealthy	0.93	0.95	0.94	600
accuracy			0.94	1200
macro avg	0.94	0.94	0.94	1200
weighted avg	0.94	0.94	0.94	1200

5.2.3 Performance Study on VGG-19 Model

35 epochs were used to train the VGG-19 model. The model demonstrated an accuracy of 65.89% and a loss of 0.6833 in the first epoch. Accuracy, recall, precision, and both training and validation losses increased over the course of the next epochs. Among the noteworthy findings is the dynamic adjustment of the learning rate, which at epoch 29 drops to 0.0001. One popular method for maximizing model convergence is this adaptive learning rate. The validation set continuously showed improved metrics, indicating the improved capacity of the model to generalize to unknown data: accuracy, recall, and precision.

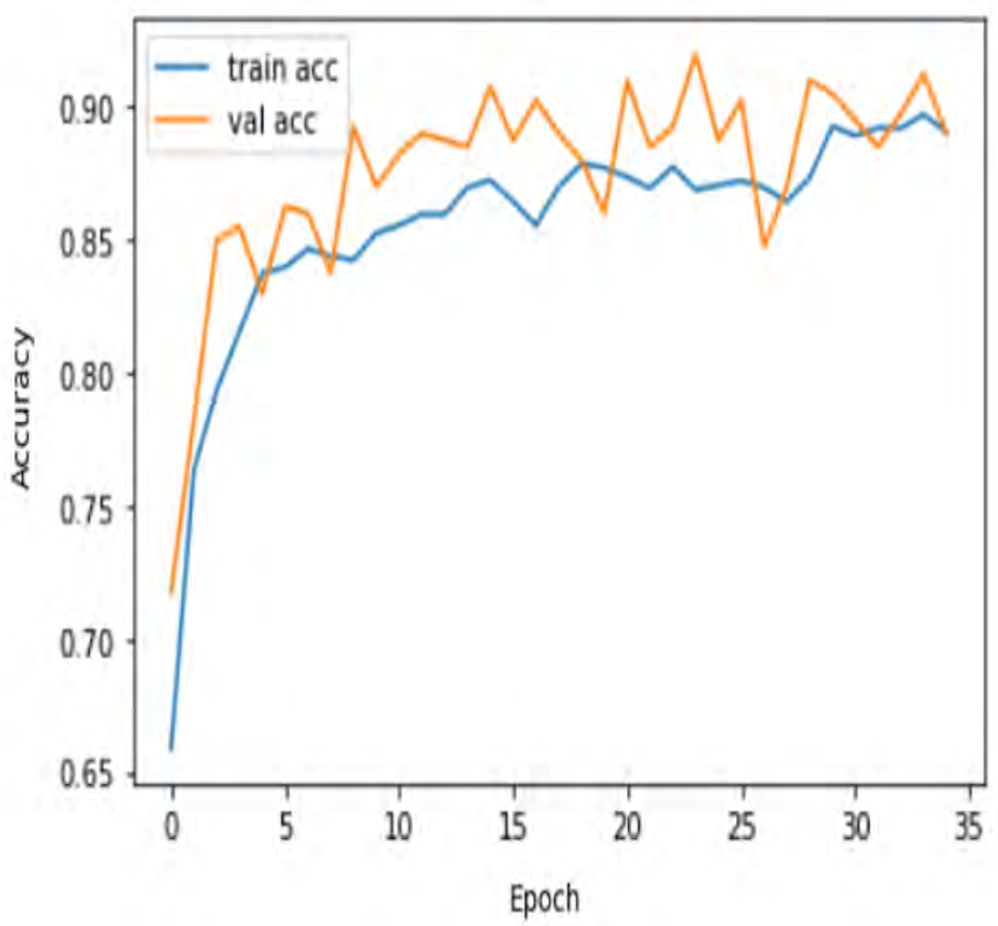

Figure 5.5: Accuracy Graph obtained from applying only VGG-19 Model

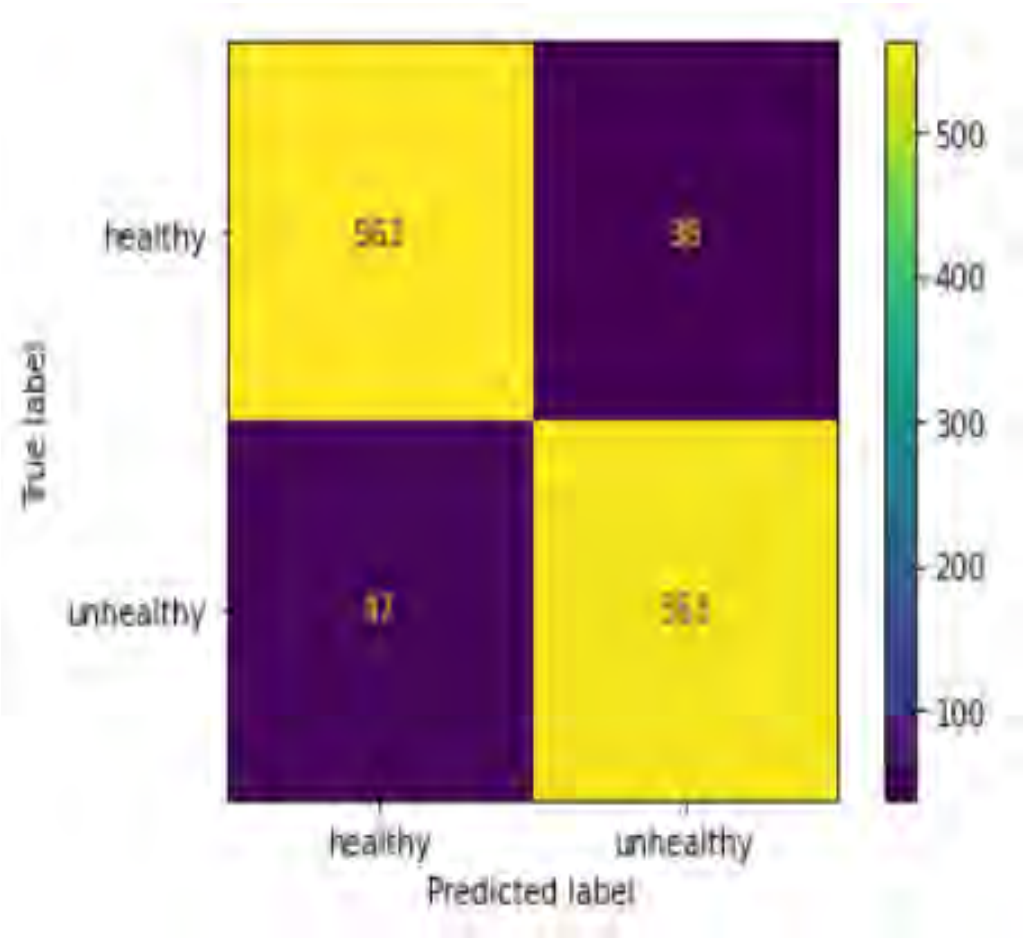

Figure 5.6: Confusion Matrix of VGG-19 Model

Table 5.3: Precision, recall and f1-score of VGG-19 Model

	precision	**recall**	**f1-score**	**support**
healthy	0.92	0.94	0.93	600
unhealthy	0.94	0.92	0.93	600
accuracy			0.93	1200
macro avg	0.93	0.93	0.93	1200
weighted avg	0.93	0.93	0.93	1200

5.2.4 Performance Study on MobilenetV3 Model

Thirty-five epochs were dedicated to training the MobileNetV3 model. Numerous performance metrics showed a steady improvement over these epochs. At the beginning of the epoch the model showed an accuracy of 80.06% and a loss of 0.7526. As Our training Accuracy increased and the loss of the data went down as a result F1 score , recall, and precision all are performed good. One noteworthy finding is that at epoch 12, the learning rate dropped to 0.0001, suggesting the use of an adaptive learning rate strategy. This adjustment most likely made it possible for the model to converge successfully. Improved metrics like accuracy, recall, and precision were consistently shown in the validation set, indicating the model's potential for good generalization to untested data.

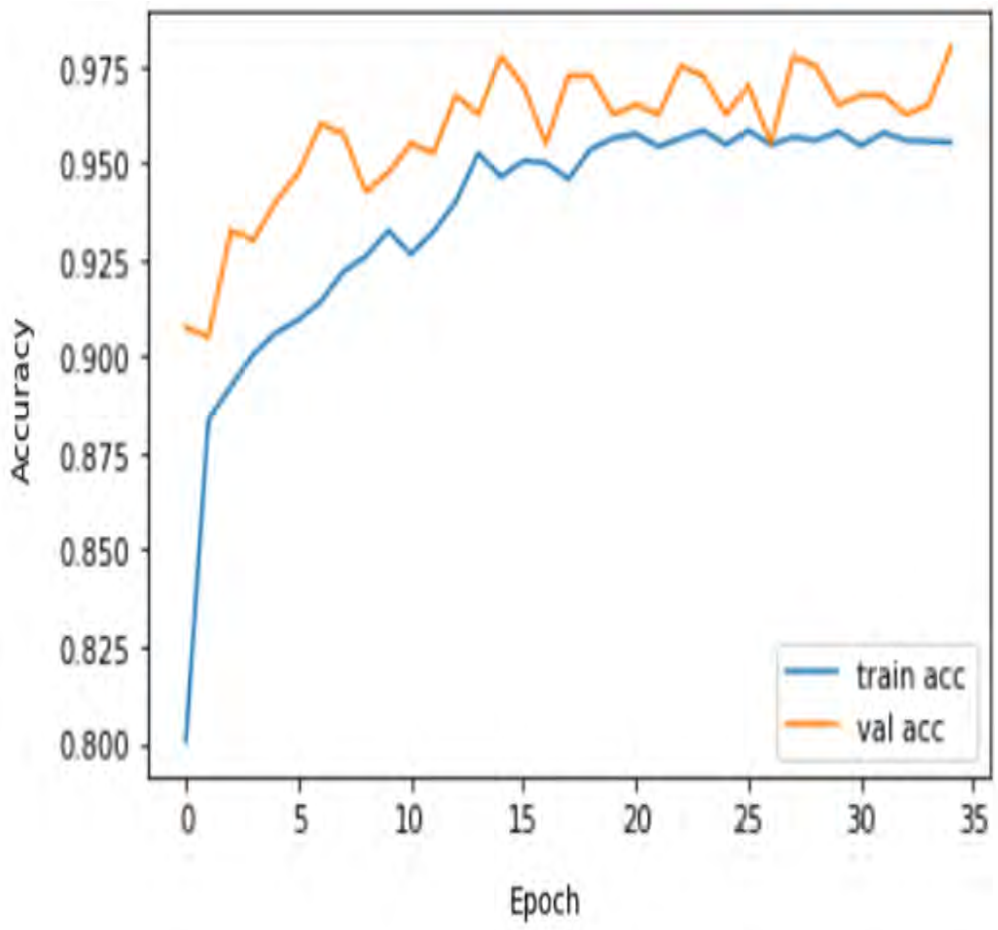

Figure 5.7: Accuracy Graph obtained from applying only MobileNetV3 Model

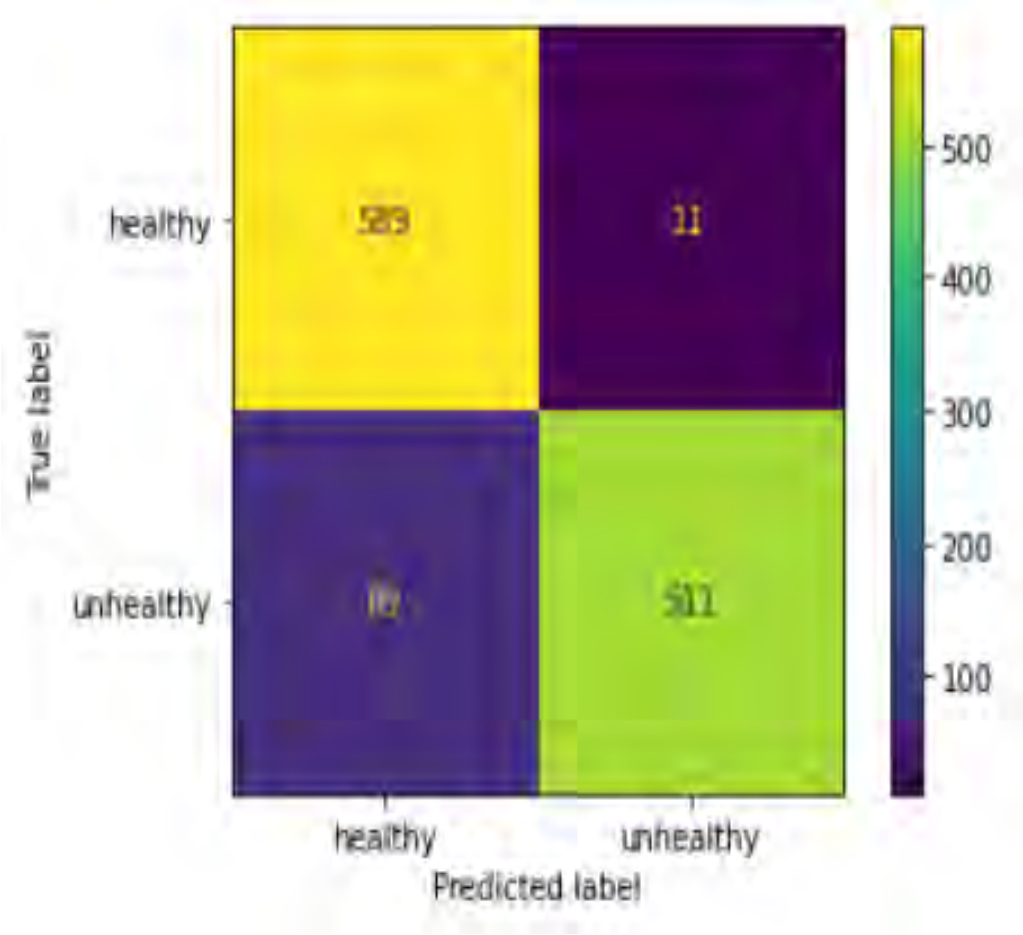

Figure 5.8: Confusion Matrix of MobileNetV3 Model

Table 5.4: Precision, recall and f1-score of MobilenetV3 Model

	precision	**recall**	**f1-score**	**support**
healthy	0.87	0.98	0.92	600
unhealthy	0.98	0.85	0.91	600
accuracy			0.92	1200
macro avg	0.92	0.92	0.92	1200
weighted avg	0.92	0.92	0.92	1200

5.2.5 Performance Study on ResNet50 Model

During the ResNet50 model's 35-epoch training process, the starting conditions demonstrated a 52.08% accuracy and a loss of 0.7311. As the model developed, the accuracy stayed around 50.14% and the loss progressively dropped to 0.6933. Starting at 0.001, the learning rate changed dynamically over the course of training, finally settling at a minimum of 1e-06. The validation metrics showed variations over the course of the epochs, with variations in the values of Recall, and Precision. A variety of learning rate reductions, the model's performance on the validation set slowed down, indicating that either more progress may be difficult to achieve or that parameters may need to be fine-tuned.

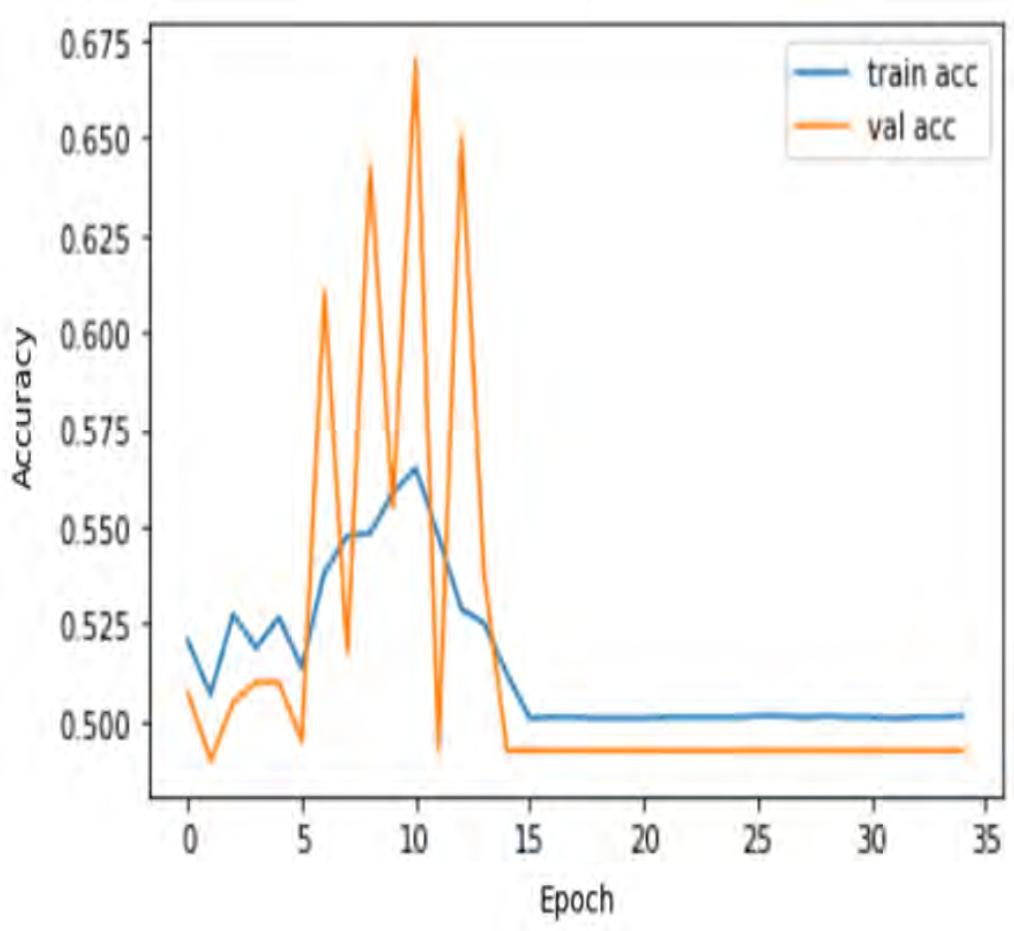

Figure 5.9: Accuracy Graph obtained from applying only ResNet50 Model

Table 5.5: Precision, recall and f1-score of ResNet50 Model

	precision	**recall**	**f1-score**	**support**
healthy	0.00	0.00	0.00	600
unhealthy	0.50	1.00	0.67	600
accuracy			0.50	1200
macro avg	0.25	0.50	0.33	1200
weighted avg	0.25	0.50	0.33	1200

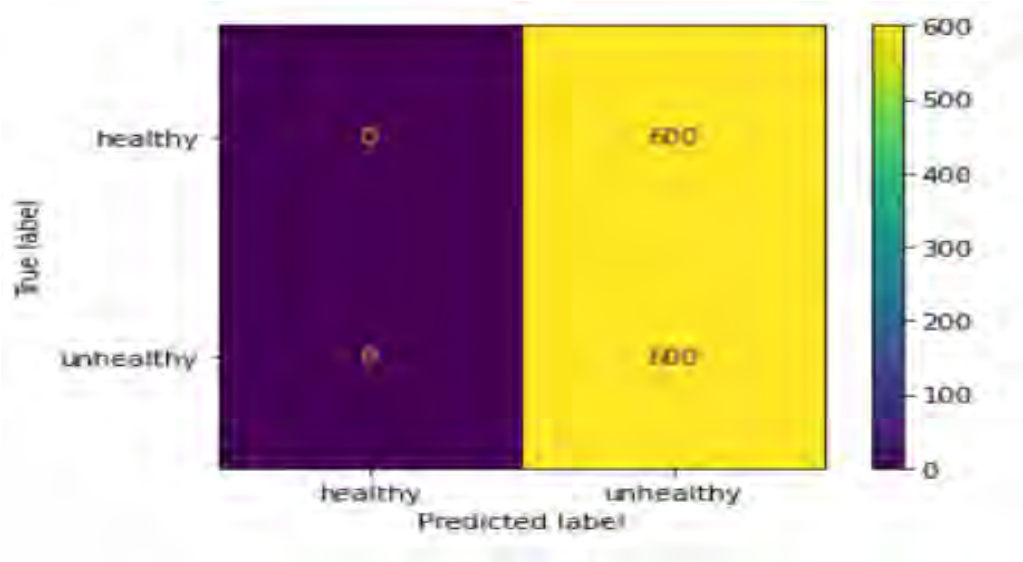

Figure 5.10: Confusion Matrix of ResNet50 Model

5.2.6 Performance Study on Ensemble Model

The model's 20 training epochs showed robust performance, starting with a training loss of 0.4162 and 96.83% accuracy. As training progressed, it reached 93.02% accuracy by the 20th epoch, with a minimum loss of 0.1634. The validation set showed a positive trend, with high accuracy of 97.25% and a decrease in loss from 0.4550 to 0.1820, indicating strong generalization ability. The model's effectiveness in producing precise predictions on fresh data is evident.

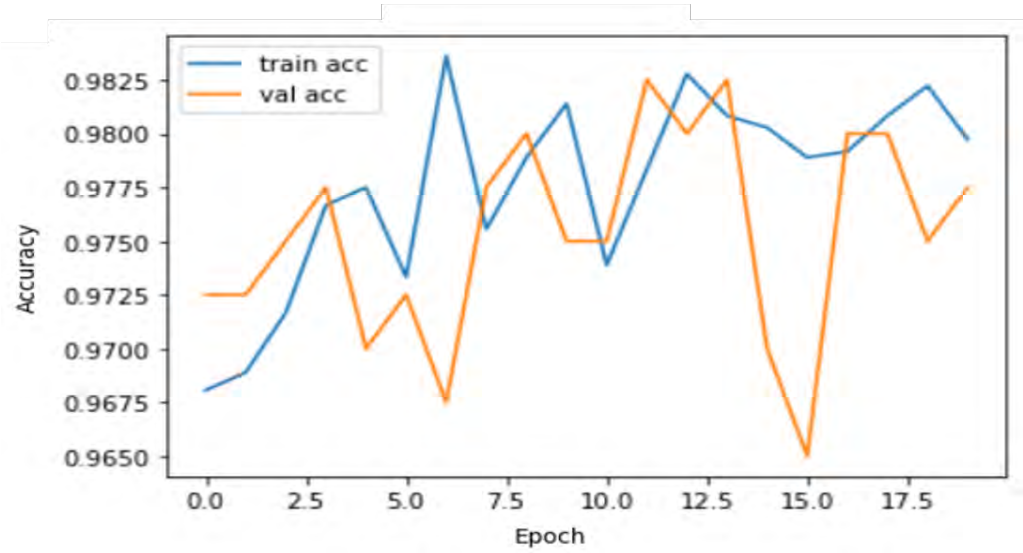

Figure 5.11: Accuracy Graph obtained from applying only Ensemble Model

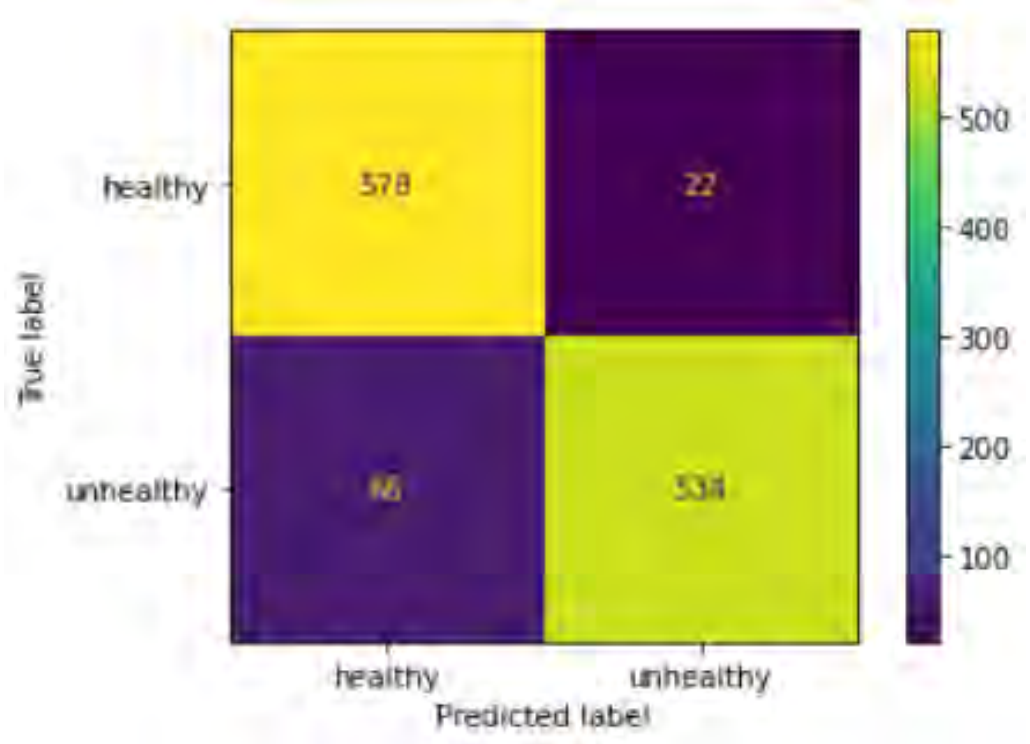

Figure 5.12: Confusion Matrix of Ensemble Model

Table 5.6: Precision, recall and f1-score of Ensemble Model

	precision	**recall**	**f1-score**	**support**
healthy	0.90	0.96	0.93	600
unhealthy	0.96	0.89	0.92	600
accuracy			0.93	1200
macro avg	0.93	0.93	0.93	1200
weighted avg	0.93	0.93	0.93	1200

5.2.7 Discussions

A comparative analysis of the different models outputs provides important insights into how appropriate each model is for the particular task. The Customized CNN performed better than the majority of the other models, exhibiting a low loss of 0.11 and a noteworthy accuracy of 95%. This implies that the architecture created especially for the task at hand showed exceptional learning capabilities and successfully identified the underlying patterns in the data.
VGG16 outperformed the other models with an impressive accuracy of 94%; Ensemble Model and VGG19 came in same position respectively, with accuracies of 93% .Mobilenet came in third position respectively, with accuracy of 92%.However, the accuracy rate of the Resnet50 were lower at 50% respectively, suggesting that Resnet50 model might have trouble understanding the complexities of the dataset.

Table 5.7: Accuracy and Loss of Models

Models	Accuracy	Healthy	Unhealthy
Customized CNN	95%	0.95	0.95
Ensemble Model	93%	0.93	0.92
VGG16	94%	0.94	0.94
VGG19	93%	0.93	0.93
MobileNet	92%	0.92	0.91
Resnet50	50%	0.00	0.67

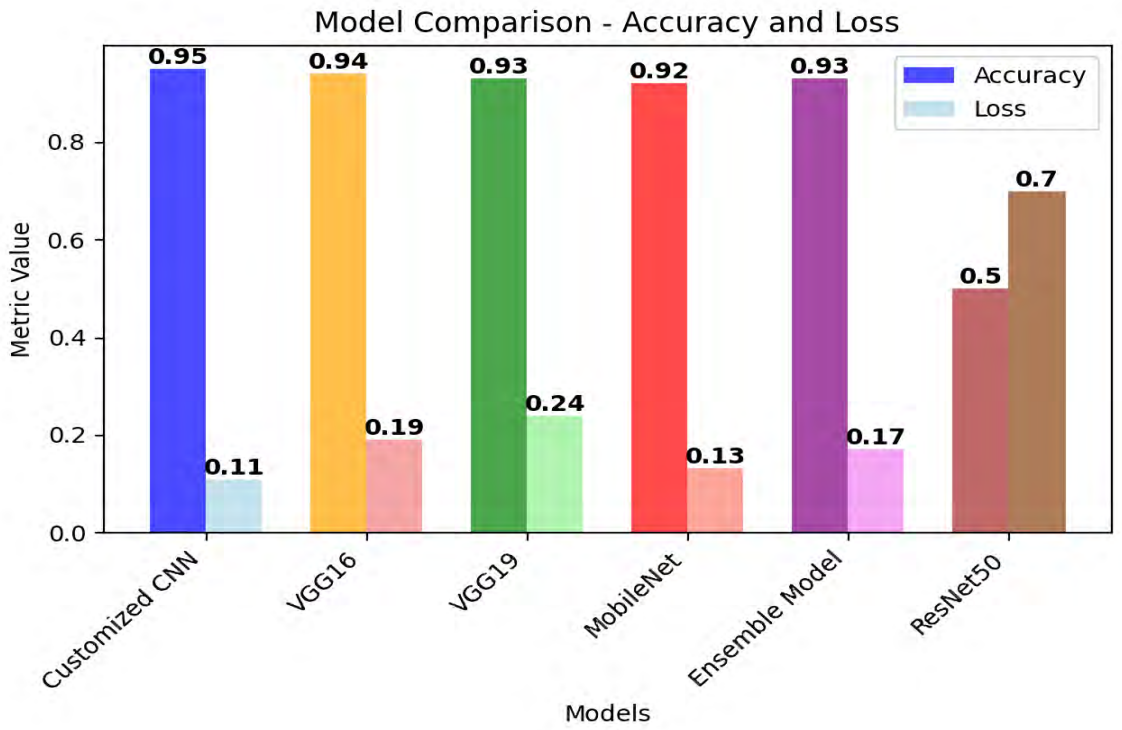

Figure 5.13: Result of models

The Customized CNN's superior accuracy when compared to all other models highlights how well the custom architecture extracts pertinent features and generates precise predictions. Even though VGG16 did well as well, the Customized CNN shows how important it is to modify the model architecture to fit the unique features of the dataset in order to achieve better performance. This emphasizes how important careful planning, design, and customization are to getting the best results possible for image classification tasks.

5.2.8 Comparison with Recent work

This thesis article compares the accuracy of ResNets implementations on fundus image datasets. Vazquez Noguera et al.[21] achieved 91% accuracy for detecting ocular diseases from color fundus images, while Parra et al.[22]achieved 93% accuracy for identifying ocular toxoplasmosis. Among all of them, our custom CNN model performs better.

Table 5.8: Work Comparison Between Recent Work

Approaches	**Models**	**Accuracy**
Customized CNN	CNN%	95%
Vazquez Noguera et.al[21]	Resnet	91%
Parra et.al.[22]	ResNets	93%

Chapter 6

Conclusion

6.1 Conclusion

Creating our proposed custom CNN model took up the most of our effort. The Ocular Toxoplasmosis dataset that has been gathered to be used for the research studies.We employ our suggested model, which consists of 860 photos split into two categories: healthy and unhealthy. In order to improve the outcome, we have expanded our dataset by adding 5200 photos.The dataset was run through four pretrained models: VGG19, VGG16, Mobilenet and Inception v3. Additionally, the OT dataset was run via our suggested CNN model, which yields higher accuracy than the models that are currently in use. Ultimately, we success to create a 16-Layer CNN model that outperforms the previous approaches that were taken into consideration.The suggested custom CNN model outraced other current models with an accuracy of 95%. With this method, ophthalmologists might be able to do efficient retinal picture analysis. This will enable them to stop blindness from occurring by starting better treatment earlier in the disease's course. As a result, in the upcoming years, we plan to make our approach more effective. As a result of receiving insufficient treatment, the patient will experience numerous physical issues.

6.2 Future Work Plan

OT is becoming a more and more common tool for treating and detecting retinal issues. It will become more user-friendly as software and technology continue to progress. Clinical utility of OT is still unknown. To compare OT's use to other imaging modalities and determine the range of retinal illnesses for which it is effective, more study is needed. Further experience and research are needed in clinical practice. To determine whether OT testing in isolation will be sufficient, more data is necessary. Furthermore, the proposed method might be used with datasets from different fields. In the future, the proposed model might be expanded to larger datasets in order to enhance its functionality even more. We will get solutions to these and other unanswered topics in a few years.

Bibliography

[1] J. S. Schuman, R. S. Weinberg, A. P. Ferry, and R. K. Guerry, "Toxoplasmic scieritis," *Ophthalmology*, vol. 95, no. 10, pp. 1399–1403, 1988.

[2] I. Cochereau-Massin, P. LeHoang, M. Lautier-Frau, *et al.*, "Ocular toxoplasmosis in human immunodeficiency virus-infected patients," *American journal of ophthalmology*, vol. 114, no. 2, pp. 130–135, 1992.

[3] G. N. Holland and K. G. Lewis, *An update on current practices in the management of ocular toxoplasmosis*, 2002.

[4] J. S. Remington, P. Thulliez, and J. G. Montoya, "Recent developments for diagnosis of toxoplasmosis," *Journal of clinical microbiology*, vol. 42, no. 3, pp. 941–945, 2004.

[5] V. Arun, A. G. Noble, T. S. Group, *et al.*, "Cataracts in congenital toxoplasmosis," *Journal of American Association for Pediatric Ophthalmology and Strabismus*, vol. 11, no. 6, pp. 551–554, 2007.

[6] E. M. Dodds, G. N. Holland, M. R. Stanford, *et al.*, "Intraocular inflammation associated with ocular toxoplasmosis: Relationships at initial examination," *American journal of ophthalmology*, vol. 146, no. 6, pp. 856–865, 2008.

[7] E. Delair, P. Latkany, A. G. Noble, P. Rabiah, R. McLeod, and A. Brézin, "Clinical manifestations of ocular toxoplasmosis," *Ocular immunology and inflammation*, vol. 19, no. 2, pp. 91–102, 2011.

[8] J. G. Garweg, J. D. de Groot-Mijnes, and J. G. Montoya, "Diagnostic approach to ocular toxoplasmosis," *Ocular immunology and inflammation*, vol. 19, no. 4, pp. 255–261, 2011.

[9] A. De-La-Torre, M. Stanford, A. Curi, G. J. Jaffe, and J. E. Gomez-Marin, "Therapy for ocular toxoplasmosis," *Ocular Immunology and Inflammation*, vol. 19, no. 5, pp. 314–320, 2011.

[10] P. Zhou, Z. Chen, H.-L. Li, *et al.*, "Toxoplasma gondii infection in humans in china," *Parasites & vectors*, vol. 4, pp. 1–9, 2011.

[11] Y.-H. Park and H.-W. Nam, "Clinical features and treatment of ocular toxoplasmosis," *The Korean Journal of Parasitology*, vol. 51, no. 4, pp. 393–399, 2013. DOI: 10.3347/kjp.2013.51.4.393.

[12] A. CDC, "Parasites-toxoplasmosis (toxoplasma infection)," *Am J Trop Med Hyg*, vol. 9, no. 1, pp. 794–799, 2014.

[13] D. P. Kingma and J. Ba, "Adam: A method for stochastic optimization," *arXiv preprint arXiv:1412.6980*, 2014.

[14] A. Jamal, M. Hazim Alkawaz, A. Rehman, and T. Saba, "Retinal imaging analysis based on vessel detection," *Microscopy research and technique*, vol. 80, no. 7, pp. 799–811, 2017.

[15] A. D. Chakravarthy, D. Abeyrathna, M. Subramaniam, *et al.*, "An approach towards automatic detection of toxoplasmosis using fundus images," in *2019 IEEE 19th International Conference on Bioinformatics and Bioengineering (BIBE)*, IEEE, 2019, pp. 710–717.

[16] Y. Elloumi, M. Akil, and H. Boudegga, "Ocular diseases diagnosis in fundus images using a deep learning: Approaches, tools and performance evaluation," in *Real-Time Image Processing and Deep Learning 2019*, SPIE, vol. 10996, 2019, pp. 221–228.

[17] A. Luque, A. Carrasco, A. Martín, and A. de Las Heras, "The impact of class imbalance in classification performance metrics based on the binary confusion matrix," *Pattern Recognition*, vol. 91, pp. 216–231, 2019.

[18] D. Abeyrathna, M. Subramaniam, P. Chundi, *et al.*, "Directed fine tuning using feature clustering for instance segmentation of toxoplasmosis fundus images," in *2020 IEEE 20th International Conference on Bioinformatics and Bioengineering (BIBE)*, IEEE, 2020, pp. 767–772.

[19] M. Hasanreisoglu, M. S. Halim, A. D. Chakravarthy, *et al.*, "Ocular toxoplasmosis lesion detection on fundus photograph using a deep learning model," *Investigative Ophthalmology & Visual Science*, vol. 61, no. 7, pp. 1627–1627, 2020.

[20] J. E. Gómez-Marín, J. Muñoz-Ortiz, M. Mejía-Oquendo, *et al.*, "High frequency of ocular toxoplasmosis in quindío, colombia and risk factors related to the infection," *Heliyon*, vol. 7, no. 4, 2021.

[21] R. Parra, V. Ojeda, J. L. Vázquez Noguera, *et al.*, "A trust-based methodology to evaluate deep learning models for automatic diagnosis of ocular toxoplasmosis from fundus images," *Diagnostics*, vol. 11, no. 11, p. 1951, 2021.

[22] R. Parra, V. Ojeda, J. L. Vázquez Noguera, *et al.*, "Automatic diagnosis of ocular toxoplasmosis from fundus images with residual neural networks.," *Public Health and Informatics*, 2021.

[23] A. Shrivastava, R. Kamble, S. Kulkarni, *et al.*, "Deep learning based ocular disease classification using retinal fundus images," *Investigative Ophthalmology & Visual Science*, vol. 62, no. 11, pp. 39–39, 2021.

[24] J. R. Smith, L. M. Ashander, S. L. Arruda, *et al.*, "Pathogenesis of ocular toxoplasmosis," *Progress in Retinal and Eye Research*, vol. 81, p. 100 882, 2021.

[25] T. Gonçalves, I. Rio-Torto, L. F. Teixeira, and J. S. Cardoso, "A survey on attention mechanisms for medical applications: Are we moving towards better algorithms?" *IEEE Access*, 2022.

[26] D. Kalogeropoulos, H. Sakkas, B. Mohammed, *et al.*, "Ocular toxoplasmosis: A review of the current diagnostic and therapeutic approaches," *International Ophthalmology*, vol. 42, no. 1, pp. 295–321, 2022.

[27] M. S. Khan, N. Tafshir, K. N. Alam, *et al.*, "Deep learning for ocular disease recognition: An inner-class balance," *Computational Intelligence and Neuroscience*, vol. 2022, 2022.

[28] E. Midena, G. Marchione, S. Di Giorgio, *et al.*, "Ultra-wide-field fundus photography compared to ophthalmoscopy in diagnosing and classifying major retinal diseases," *Scientific Reports*, vol. 12, no. 1, p. 19 287, 2022.

[29] O. Ouda, E. AbdelMaksoud, A. Abd El-Aziz, and M. Elmogy, "Multiple ocular disease diagnosis using fundus images based on multi-label deep learning classification," *Electronics*, vol. 11, no. 13, p. 1966, 2022.

[30] A. Zafar, M. Aamir, N. Mohd Nawi, *et al.*, "A comparison of pooling methods for convolutional neural networks," *Applied Sciences*, vol. 12, no. 17, p. 8643, 2022.

[31] S. Samiul Alam, S. Based Shuvo, S. Nafisa Ali, F. Ahmed, A. Chakma, and Y. M. Jang, "Benchmarking deep learning frameworks for automated diagnosis of ocular toxoplasmosis: A comprehensive approach to classification and segmentation," *arXiv e-prints*, arXiv–2305, 2023.

[32] A. A. P. Siswadi, "Computer-aided-diagnosis for ocular abnormalities from a single color fundus photography with deep learning," Ph.D. dissertation, Bourgogne Franche-Comté, 2023.

[33] *Basics of cnn in deep learning - analytics vidhya*, https://www.analyticsvidhya.com/blog/2022/03/basics-of-cnn-in-deep-learning/, (Accessed on 01/22/2024).

[34] *How to choose an activation function for deep learning - machinelearningmastery.com*, https://machinelearningmastery.com/choose-an-activation-function-for-deep-learning/, (Accessed on 01/22/2024).

[35] *Ocular toxoplasmosis fundus images dataset*, https://zenodo.org/records/4479724, (Accessed on 01/22/2024).

[36] *Toxoplasmosis - infectious diseases - msd manual professional edition*, https://www.msdmanuals.com/en-jp/professional/infectious-diseases/extraintestinal-protozoa/toxoplasmosis, (Accessed on 01/22/2024).